October 2019

The Effects of Acidosis on Calcium Dependent Binding of A Single Crossbridge

Matthew Unger

The effects of acidosis on calcium dependent binding of a single crossbridge

A Thesis Presented

By

MATTHEW P. UNGER

Submitted to the Graduate School of the

University of Massachusetts Amherst in partial fulfillment

Of the requirements for the degree of

Master of Science

September 2019

School of Public Health and Health Sciences

Kinesiology

The effects of acidosis on calcium dependent binding of a single crossbridge

A Thesis Presented

By

MATTHEW P. UNGER

Approved as to style and content by:

Edward P. Debold, Chair

Mark S. Miller, Member

Jennifer L. Ross, Member

Jane A. Kent, Department Chair
Kinesiology

ABSTRACT

THE EFFECTS OF ACIDOSIS ON CALCIUM DEPENDENT BINDING OF A SINGLE CROSS BRIDGE

SEPTEMBER 2019

MATTHEW P. UNGER, B.S., UNIVERSITY OF MASSACHUSETTS AMHERST

M.S., UNIVERSITY OF MASSACHUSETTS AMHERST

Directed by: Professor Edward P. Debold

Intracellular acidosis is a putative agent of skeletal muscle fatigue, in part, because acidosis depresses the calcium (Ca^{2+}) sensitivity and force production of muscle (18, 50). However, the molecular mechanisms behind this depression in Ca^{2+} sensitivity and force production are unknown. This gap in knowledge poses a significant challenge in generating a complete understanding of the fatigue process. To close this gap, the ability of myosin to bind to a single actin filament was measured under acidic conditions, in a laser trap assay, with and without regulatory proteins. Decreasing pH from 7.4 to 6.5 reduced the frequency of single actomyosin binding events at submaximal (pCa 8 – pCa 6), but not at maximal (pCa 5 - 4) concentrations. To delineate whether this was due to a direct effect on myosin versus an indirect effect on the regulatory proteins, troponin (Tn) and tropomyosin (Tm), binding frequency was also quantified in the absence of Tn and Tm. Acidosis did not alter the frequency of actomyosin binding events in the absence of regulatory proteins (1.4 ± 0.05 vs 1.4 ± 0.13 events/sec for pH 7.4 and 6.5). Additionally, acidosis did not significantly affect the size of myosin's powerstroke, or the duration of binding events in the presence of regulatory proteins, at every pCa. These data suggest that acidosis impedes activation of the thin filament by competitively inhibiting Ca^{2+} binding to TnC. This slows the rate at which myosin initially

attaches to actin, therefore less cross-bridges will be bound and generating force at any given sub-maximal pCa.

TABLE OF CONTENTS

LIST OF TABLES

Page

LIST OF FIGURES

Page

Chapter 1
INTRODUCTION

1.1 Skeletal muscle fatigue

Skeletal muscle fatigue is defined as a decrease in the force or power generating capacity of muscle in response to repetitive contractile activity (32, 66). There is strong evidence that suggests fatigue, which develops as a result of short-term, high intensity exercise, occurs within the muscle (45). However, the mechanisms which explain this phenomena are still incomplete (1). Despite the lack of mechanistic insight, multiple factors have been identified in playing a role in this type of fatigue. Of those, acidosis, or elevated proton (H^+) concentration, is thought to play a direct role in the development of fatigue, but the molecular mechanisms responsible for this effect remain unclear.

Studies using ^{31}Phosphorous-Magnetic Resonance Spectroscopy, a method for measuring biochemical changes in muscle demonstrate that several alterations occur in the muscle during contractile activity including an increase in Pi and H^+ (47). This work also established a temporal correlation between the development of muscle fatigue and H^+ accumulation in contracting muscle (47). Parallel efforts using skinned single skeletal muscle fibers provided evidence of a causative link between acidosis and depressions in contractile performance (10, 18, 35, 46). Specifically, these efforts have suggested that acidosis may be responsible for a moderate decrease in maximum tension at saturating calcium (Ca^{2+}) levels, a substantial reduction in unloaded shortening velocity, and a pronounced reduction in Ca^{2+} sensitivity (10, 35, 49, 56). Figure 1 shows one conceptual framework of how acidosis might elicit its effects on muscle function during fatigue.

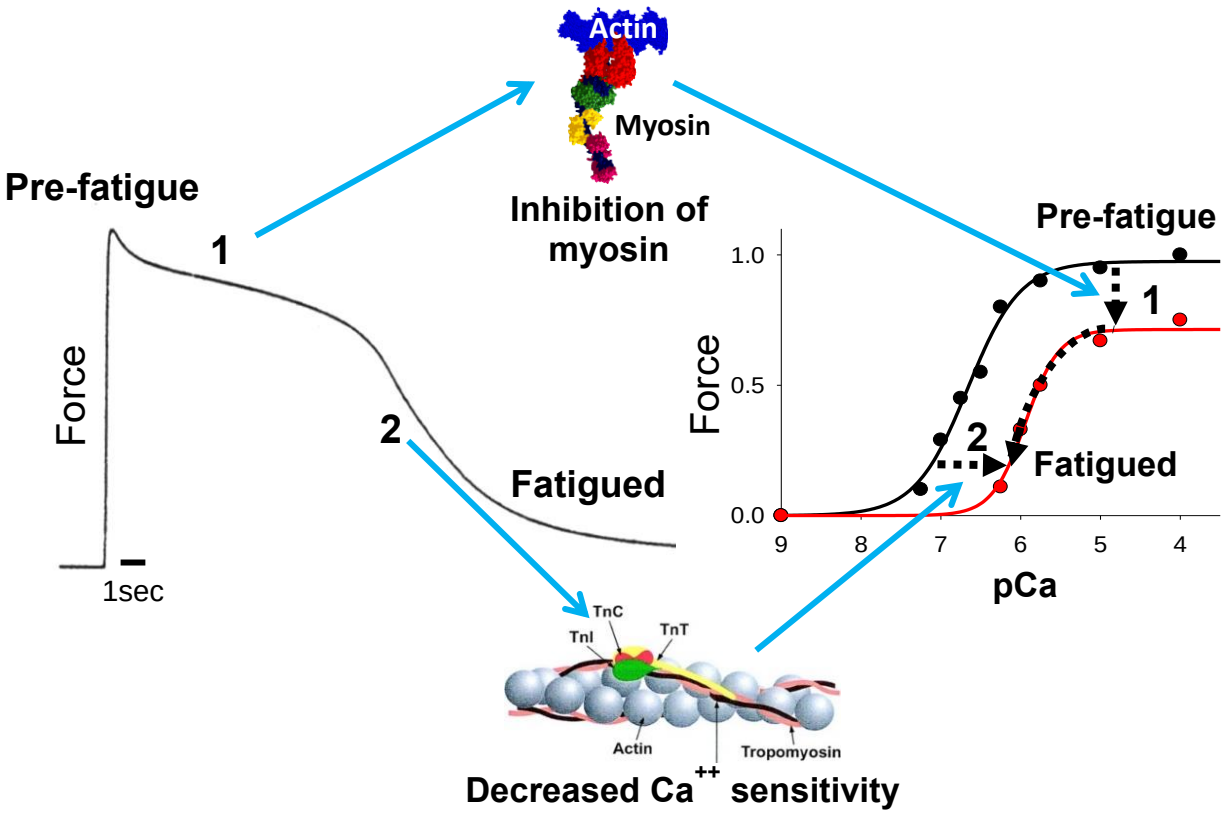

Figure 1 Conceptual framework highlighting the possible mechanisms of fatigue. On the left, a force record from a fatigue protocol (71). The initial declines in force production of isolated muscle tissue (**1**) are thought to be mediated through direct effects on myosin (70). The steep drop seen later in fatigue (**2**) is a result of the fatigue induced depression in Ca^{2+} sensitivity combined with a decreased release of Ca^{2+} from the sarcoplasmic reticulum (SR) (1). The graph on the right illustrates how the combination of both effects dramatically decreases force production at sub-saturating Ca^{2+} concentrations.

Many of the single muscle fiber studies which found impairments in contractile performance of muscle measured the effect of H^+ accumulation at saturating levels of free Ca^{2+} and thus with a fully activated thin filament (10, 22, 33). This leads to the conclusion that the effects of acidosis, are in part, due to direct effects on the actomyosin crossbridge, (see #1 Fig. 1) (70). For this

reason, the goal of recent work has been to determine which steps in the crossbridge cycle are impacted by acidosis (Figure 2). One such study determined myosin's ADP-release step of the

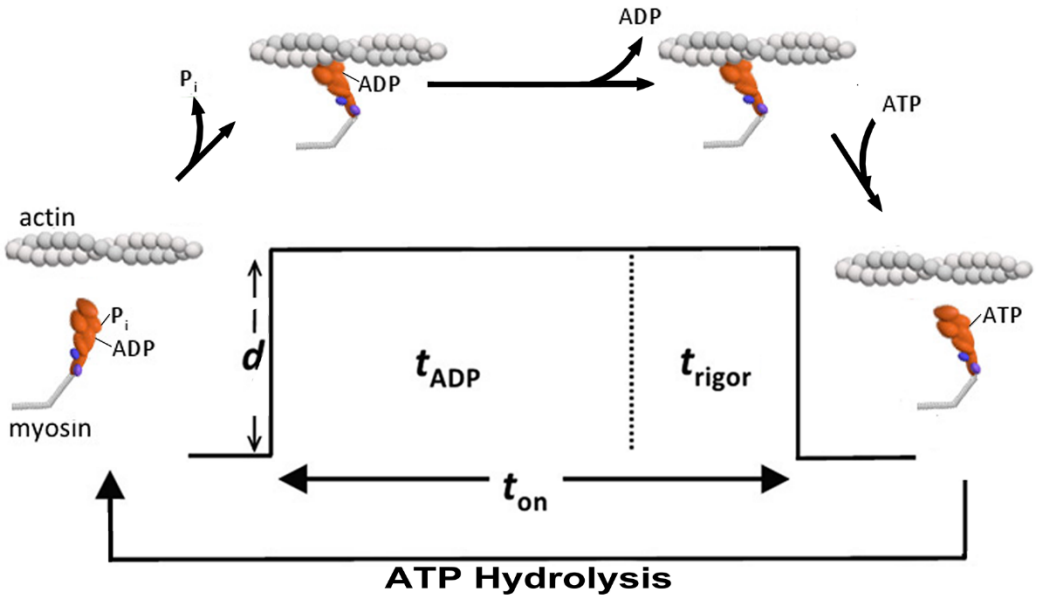

Figure 2 The current scheme indicating the steps of the crossbridge cycle. The cycle begins in the weakly bound M*ADP*Pi state. This is followed by a weak to strong binding transition to AM*ADP*Pi with Pi release occurring rapidly. Once Pi is released, myosin undergoes its lever arm rotation causing actin displacement and force production. Post power-stroke, myosin is still strongly bound to actin in the AM*ADP state. Following a non-reversible isomerization step, ADP is released leaving myosin and actin in the AM rigor bond state. Once a new ATP binds to myosin, the AM rigor bond is dissociated leaving myosin in the M*ATP state. ATP hydrolysis quickly follows this step. **d** represents the myosin's inherent step size and $\mathbf{t_{on}}$ represents the time myosin remains strongly bound to actin. Figure from (15).

crossbridge cycle is slowed by approximately 66% as a result of acidosis (12). An outcome that

provides a compelling explanation for the decreased contraction velocity caused by fatigue *in vivo*. Additional studies which investigated the effects of acidosis on actin activated myosin ATPase found a 90% reduction in the rate of ATP hydrolysis at pH 6.5 compared to pH 7.4 (71), indicating there are possibly other steps of the crossbridge cycle slowed by acidosis which could possibly decrease the number of strongly bound crossbridges (71). A result which provides a possible explanation for the small decreases in isometric tension seen in single muscle fiber studies (#1 in Figure 1). To account for the more dramatic drop in muscle performance, one must also consider the acidosis induced depression in Ca^{2+} sensitivity of the regulated thin filament (RTF) (18), which, when combined with the loss of Ca^{2+} release from the sarcoplasmic reticulum (SR) late in fatigue (70), has a dramatic impact on muscle performance (see #2 in Figure 1). Therefore, the goal of follow up studies was to determine the mechanisms responsible for the acidosis induced depression in Ca^{2+} sensitivity of the thin filament (38, 53, 55). One possible reason that explains the apparent decrease in Ca^{2+} sensitivity is that troponin (Tn) seems to lose its affinity for Ca^{2+} under acidic conditions. Troponin is a globular protein with three distinct subunits; TnC, the Ca^{2+} binding subunit, TnI, the inhibitory subunit and TnT, the Tm binding subunit (19, 48, 65). Therefore researchers hypothesized that Tn loses its affinity for Ca^{2} under acidic conditions, possibly due to H^{+} ions competitively binding to the Ca^{2+} TnC(55). Subsequent studies that used chimeras of Tn, found that the pH induced depressions of cardiac TnC (cTnC) affinity for Ca^{2+} partially improved when cardiac TnI (cTnI) or cardiac TnT (cTnT) were replaced with skeletal TnI (sTnI) and/ or skeletal TnT (sTnT) (38). Evidence that TnI and TnT play a role in the depressed Ca^{2+} sensitivity caused by acidosis. Additional studies

highlighted the importance of Tn structure by demonstrating that point mutations in either sTnC or sTnI could partially ameliorate the acidosis induced depression in Ca^{2+} sensitivity (40).

The mechanisms responsible for the both the direct and indirect effects of acidosis on crossbridge function are becoming clearer. However, because many of these studies were performed in muscle fibers, the observed result represents the cumulative action of acidosis on billions of actomyosin crossbridges. Thus, there is a need to observe the effects of acidosis on single actomyosin interactions. Due to developments in the field of muscle biophysics, the mechanics and kinetics of Ca^{2+} regulated actomyosin interactions can be quantified (30, 39, 64).

The goal of this proposal is to investigate the underlying molecular mechanisms responsible for the precipitous drop in contractile performance of muscle in response to acidosis. With emphasis put on the combined effects of acidosis and decreased Ca^{2+} release from the SR (Figure 1). Since this study will be performed at the single molecule level, both with and without regulatory proteins, the direct effects of acidosis on myosin (#1 in Figure 1) will be delineated from the effects of acidosis on the RTF (#2 in Figure 1). This will allow us to investigate the molecular mechanism responsible for the acidosis-induced decrease in Ca^{2+} sensitivity and force production in muscle fibers from the perspective of single actomyosin crossbridge.

Chapter 2
LITERATURE REVIEW

2.1 The link between acidosis and fatigue

During intense contractile activity, increased rates of ATP hydrolysis and glycolysis lead to an accumulation of H^+ which decreases intramuscular pH from resting levels of ~7.0 to 6.5 and in extreme cases to 6.2 (47). As pH decreases from resting levels to those observed during fatigue, maximum force output *in vivo* decreases by as much as 70% (47). However, because ^{31}P-MRS studies are performed *in vivo*, the measured reduction in force is most certainly a result of the combined effects of H^+, Pi, ADP and reactive oxygen species (ROS) (13). Thus, the role that acidosis plays in fatigue cannot be determined independently of these other metabolic biproducts. Parallel efforts, using chemically skinned rabbit psoas muscle fibers, determined that decreasing pH from 7.0 to 6.2 was enough to decrease peak isometric tension (P_o) and maximum contraction velocity (V_{max}) by ~30% at 15˚C in saturating pCa (8, 10). These results suggest that acidosis is playing some causative role in skeletal muscle fatigue.

The observation that acidosis depresses isometric tension and contraction velocity in fully activated muscle fibers, i.e. in saturating Ca^{2+}, at 10˚C was an indication that H^+ ions are acting directly on the actomyosin crossbridge (70). However, when similar studies were performed at near *in vivo* temperatures (30˚C), Peak isometric tension (P_o) only decreased by 4 - 18% at pH 6.2 in rat muscle fibers (35, 56). Because the effects of pH on P_o seemed to be mitigated at 30˚C under saturating Ca^{2+}, many researchers questioned the role of acidosis in fatigue (56). However, because myoplasmic Ca^{2+} concentrations decrease from ~pCa 5.3 to ~6.3 after 2 - 3 minutes of high frequency stimulation (36, 70), reviewed in (1), the acidosis induced

decrements in crossbridge function at saturating Ca^{2+} concentrations may only be representative of what occurs early in fatigue (47). Therefore, to more accurately simulate later stage fatigue, the tissue needs to be exposed to excess H^+ ions and be activated with submaximal concentrations of Ca^{2+}. Indeed, when rat muscle fibers are exposed to pH 6.2 and activated with submaximal Ca^{2+} concentrations at 30˚C, the reductions in P_o are considerably larger when compared to fibers activated with maximal Ca^{2+} concentrations (50). Therefore, the acidosis induced decrements in crossbridge function under submaximal Ca^{2+} conditions are more representative of what occurs during later stage fatigue. The reduced RTF Ca^{2+} sensitivity manifests as a rightward shift in the force-pCa relationship (Figure 1, right panel), which, when combined with the decreased myoplasmic Ca^{2+} concentration observed late in fatigue, can have severe detriments on muscle performance (70).

Although the development of skeletal muscle fatigue is in part caused by decreased Ca^{2+} release from the SR and other compounds such as Pi, ADP, and reactive oxygen species (ROS) are implicated in the fatigue process (1), the link between acidosis and muscle fatigue remains strong. This proposal will focus on quantifying how acidosis impacts actomyosin interaction. Specifically, how does acidosis impact the mechanics and kinetics of actomyosin interactions in the absence of regulatory proteins and then in a Ca^{2+} regulated system at low pH.

2.2 Mechanism of Activation

When observing actomyosin interactions in a Ca^{2+} regulated system one must consider the activation state of the RTF which, includes actin, Troponin (Tn), and Tropomyosin (Tm). While there is a cascade of events that must occur within the neuromuscular system for muscle

contraction to occur (17, 59), the focus of this proposal is on the RTF and its role in regulating actomyosin interaction. Specifically, how the direct effects of acidosis on myosin, and on the RTF affect actomyosin interaction at submaximal Ca^{2+} concentrations.

2.2.1 The Regulated Thin Filament (RTF)

The actin filament is decorated with two regulatory proteins; troponin (Tn) and tropomyosin (Tm). Troponin and Tm work with one another to regulate muscle contraction in a Ca^{2+} dependent manner. Troponin is a globular protein with three distinct subunits; TnC, the Ca^{2+} binding subunit, TnI, the inhibitory subunit and TnT, the Tm binding subunit (19, 48, 65). Tropomyosin is a 42 nm long, filamentous coiled-coiled protein that assembles into a continuous-flexible-chain that can extend the length of an actin filament (60). In a relaxed muscle, i.e. in the absence of Ca^{2+}, the Tm cable assembly blocks myosin binding sites on actin. Before actomyosin binding and subsequent force production can occur, Ca^{2+} must be released by the sarcoplasmic reticulum and bind to TnC.

Previously, researchers believed that Ca^{2+} activation worked as an "on – off" switch, i.e. as soon as Ca^{2+} is released from the SR, the muscle is completely activated. Instead, the process of activation is best modeled as a three-state system. McKillop & Geeves (1993) first presented the need for the 3-state model of regulation in favor of a 2-state model because Mckillop & Geeves (1991) found two distinct populations of RTF in the "off-state", one of which had a higher affinity for myosin than the other, which clearly disagrees with a 2-state model. This led them to believe that these two "off-states" must be two distinct populations and thus, the 3-state model was introduced (43, 44). Ultimately, they describe a model where the position of the Tm cable assembly exists in a dynamic equilibrium between 3 positions. When no Ca^{2+} is

present, Tm is in a blocked position. This keeps strong-binding sites obscured from myosin's view, thereby keeping the muscle in a relaxed state. When Ca^{2+} binds to Tn, Tm moves to the closed position. This allows for partial exposure of myosin strong binding sites and increases myosin's binding rate 50 fold (39). When the initial myosin head binds, myosin pushes Tm into the open state, thereby fully activating the thin filament. Because Tm exists as a continuous flexible chain, researchers believe that myosin binding forces neighboring Tm into the open state thereby locally activating the thin filament. This local activation can extend up to 400 nm away, thus accelerating the binding rate of neighboring myosin heads up to 10 fold in a cooperative binding process (16, 39, 57). This cooperativity causes the force-pCa relationship to have the steep sigmoidal shape (Figure 1, right panel). The molecular representation of the current 3-state model can be seen below (Figure 3) (24, 43).

The activation of muscle is a complicated process that relies on the close communication of Tn, Tm and actomyosin binding. Because fatigue-induced-acidosis is known to impact actomyosin binding through direct effects on myosin and on the RTF, there is a possibility that acidosis mediates at least some of the detrimental effects through each of these systems.

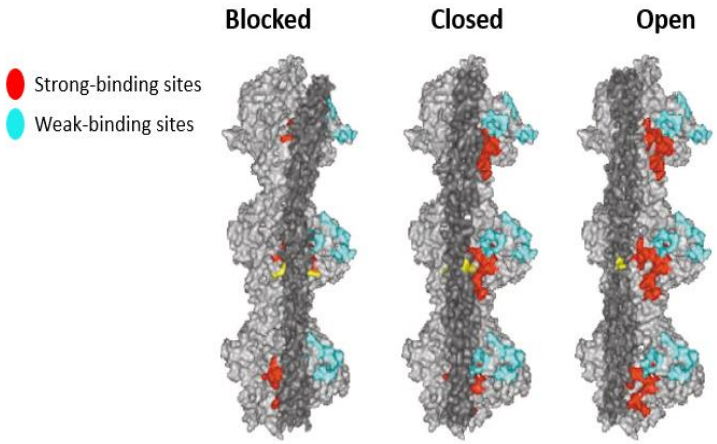

	% Time in each state	% Time in each state	% Time in each state
No Ca^{2+}	~ 76%	~ 22%	≤ 2%
Saturated Ca^{2+}	≤ 5%	~ 80%	~ 20%

Figure 3 3-D reconstruction of the 3-state model indicating blocked closed and open positions of Tm (22). Actin (grey), has strong binding sites (red) and weak binding sites (cyan). Tm (black) resides in three distinct positions on actin; (1) a blocked position where strong binding sites are completely blocked, (2) a closed position where strong binding sites are partially revealed and (3) an open position where strong binding sites are completely available. The table below the 3-D model indicates the relative percent of filaments in the 3-states in the absence and presence of Ca^{2+}. Data from (43).

2.3 Fatigue-induced-acidosis: Effects on the Regulated Thin Filament

The reduction in RTF Ca^{2+} sensitivity in response to acidosis, well characterized in skinned single muscle fibers (18, 50), is thought to play an important role when myoplasmic Ca^{2+} concentration is compromised because of decreased release from the SR (70). This decreased Ca^{2+} release from the SR only accounts for a small reduction in contractile performance of pre-fatigued muscle, rather, the combined effects of H^+ on Ca^{2+} sensitivity combined with decreased myoplasmic Ca^{2+} concentration leads to the severe reductions in contractile performance of skeletal muscle several minutes into the fatigue process (70).

Because Tn is the protein responsible for Ca^{2+} binding, many studies have investigated how acidosis impacts TnC-Ca^{2+} binding as well as how the transmission of the Ca^{2+} binding signal is affected by acidosis. To determine what role Tn may play in the desensitization of the RTF in response to acidosis, Parsons et al. (1997) devised a method to simultaneously measure TnC-Ca^{2+} binding and force production of skinned cardiac and skeletal muscle fibers. By removing endogenous skeletal TnC (sTnC) or cardiac TnC (cTnC) and replacing them with a fluorescently labeled construct; either $sTnC_{DANZ}$ or $cTnC_{IAANS}$, Parsons and colleagues were able to track Ca^{2+} binding to TnC via fluorescence changes of $sTnC_{DANZ}$ and $cTnC_{IAANS}$ that occur during Ca^{2+} binding, where higher amounts of fluorescence correspond to greater Ca^{2+} binding. They found that when the pH of the activation buffer was decreased from 7.0 to 6.5 there was a rightward shift in the force-pCa relationship as well as a rightward shift in the fluorescence-pCa relationship. A decrease in the pCa_{50} (the concentration of Ca^{2+} to get to 50% of the maximum activation) was observed for both force and fluorescence in the skeletal and cardiac muscle fibers. These results indicate that Ca^{2+} binding to TnC as well as tension development is

decreased in response to acidosis. Parsons et al. (1997) speculated this was caused by H^+ competitively binding to TnC. Because the affinity of TnC to Ca^{2+} is enhanced by strongly bound myosin (5, 63), Parsons et al. (1997) performed the same experiments in the presence of 2, 3-Butanedione monoxime (BDM), a compound that stabilizes the weakly bound state of myosin. When performed in the presence of BDM, the maximum force development in both skeletal and cardiac fibers decreased by ~24%. However, there were no changes in the fluorescence response, an indication that the pH-induced changes in the fluorescence-pCa relationship were primarily related to changes in Ca^{2+} binding to cTnC or sTnC (55). Parsons and colleagues also speculated that the rightward shift in the force/fluorescence-pCa relationship could be a result of altered transmission of the TnC-Ca^{2+} binding signal.

Recent advances in our understanding of the molecular motions responsible for transmission of the TnC-Ca^{2+} binding signal are revealing much of the detail of this process. For instance, in the absence of Ca^{2+}, the inhibitory subunit of Tn (TnI) holds Tm in a position that sterically blocks myosin strong binding to actin (65). Calcium binding to TnC reveals a hydrophobic patch in the N-terminus of TnC that biases the C-terminal region of TnI toward TnC (Figure 4). This movement of TnI toward TnC releases the steric constraints previously placed on Tm (21). Tropomyosin is then free to occupy a position that allows myosin to bind actin, first weakly then strongly, thereby fully activating the thin filament (43). This weak to strong binding transition is thought to be the step in the crossbridge cycle regulated by Ca^{2+} (23). Because myosin strong binding is required to fully activate the thin filament, the apparent loss of Ca^{2+} sensitivity in response to acidosis, could be due, in part, to direct effects on myosin. However, when strong binding is inhibited via BDM, the affinity of TnC to Ca^{2+} is still impaired (55). This

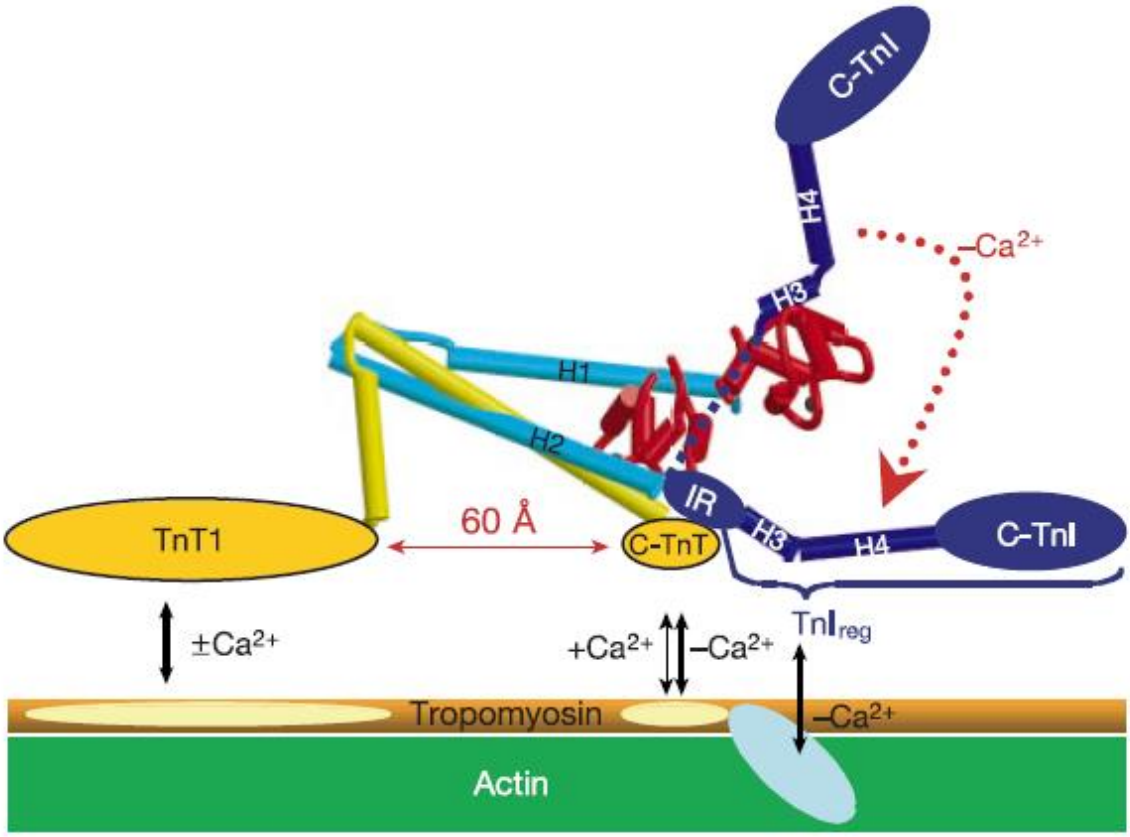

Figure 4 A ball and stick model of the 3-subunit Tn complex. The black-bolded arrows indicate a strong interaction between two subunits while thinner-black arrows indicate a weaker interaction. $+Ca^{2+}$ indicates the addition of Ca^{2+}, $-Ca^{2+}$ indicates the absence of Ca^{2+} and lastly $\pm Ca^{2+}$ indicates the interaction is unchanged by Ca^{2+} concentration. In the absence of Ca^{2+}, $-Ca^{2+}$, C-TnI is biased toward Tropomyosin (beige) causing actomyosin binding sites to be obscured, leaving the thin filament deactivated. Figure from (65).

does not rule out the possibility that direct effects of acidosis on myosin can impact Ca^{2+} sensitivity, however, these findings do indicate that Tn plays a role in the decreased Ca^{2+} sensitivity in response to acidosis. However, there is also evidence for a role of TnI in the acidosis-induced decrease in Ca^{2+} sensitivity of cardiac muscle (4), where the greater

susceptibility of cardiac fibers to acidosis was improved if cTnC and/ or cTnI were replaced with fast skeletal TnC and/ or TnI. Other studies have since corroborated these findings (38). Gaining deeper insight into the molecular motions of Tn is crucial for understanding how these motions are affected by acidosis and subsequently how acidosis affects Ca^{2+} activation.

Because muscle activation also relies on the movements of Tm over the surface of actin, other researchers have focused on Tm dependent effects of acidosis. By removing endogenous RTF from bovine cardiac fibers with gelsolin and reconstituting them with either cardiac Tm (cTm) and sTn, or sTm and cTn, Fujita and Ishiwata (1999) demonstrated that active tension was lower in cardiac fibers with cTm compared to cardiac fibers with sTm in low pH buffer (20). This depressive effect on tension development was independent of the type of Tn used, evidence that Tm plays an active role in the depression of force generation associated with fatigue-induced-acidosis. Despite Tm's role in tension development, the role Tm plays in the decreased Ca^{2+} sensitivity of the RTF is less clear. Recent studies utilizing advancements in transgenic mouse models have provided insight into the possible role Tm plays in decreased Ca^{2+} sensitivity. A common familial hypertrophic cardiomyopathy (FHC) mutation in cTm (Tm-E180G) imparts increased Ca^{2+} sensitivity to cardiac myofilaments in low (6.9) and high pH buffer (7.4) compared to non-transgenic mice (61). This enhanced Ca^{2+} sensitivity leads to hyper contractility, myocardial ischemia and often results in sudden cardiac death (42). Because Tm-E180G resides in the region where Tm interacts with TnI and actin (6, 37), the idea that a mutation here impacts the transmission of the Tn-Ca^{2+} binding signal as well as the movement of Tm over the surface of actin is plausible. New findings from studies investigating the basic

mechanism underlying RTF activation provide invaluable insights to probe our understanding of how acidosis, or other fatiguing agents mediate the effect of decreased Ca^{2+} sensitivity.

2.3.1 – Acidosis-induced-fatigue: Effects on Actomyosin interaction

In addition to the indirect effects of acidosis on actomyosin interaction that are mediated through the RTF, there are also direct effects of acidosis on actomyosin interaction (70). These direct effects work to inhibit the force, power and motion generating capacity of myosin (10). Because the force, power and shortening velocity generated by muscle ultimately depends on the cyclic interaction of myosin and actin known as the crossbridge cycle (28), many researchers focused on determining which steps in the cycle (Figure 2) are affected by acidosis.

Early work using isolated myosin preparations identified that hydrogen ion (H^+) release is closely coupled to the ATP hydrolysis step and Pi release step Because H^+ ions are involved in these steps (2, 9), researchers postulated that excess H^+ accumulation that occurs during fatigue could be impacting ATP hydrolysis and Pi release. Additionally, because both steps occur either off actin or prior to strong-binding, slowing them would decrease the rate of attachment, thereby decreasing the number of strongly attached crossbridges, ultimately decreasing force production (28, 67). This is consistent with single fiber studies where force generation is decreased at 20˚C (10) and 30˚C (56); although the acidosis induced reductions in force are less severe at higher temperatures when activated with maximum Ca^{2+} concentrations.

In addition to the direct effects of acidosis on myosin that cause detriments in force production, there is also a severe decrease in unloaded shortening velocity. In skinned muscle

fiber preparations, decreasing pH from 7.0 to 6.2 reduces maximal shortening velocity by ~20 – 30% at near physiological temperatures (31, 35). Other studies using purified myosin and actin in an *in vitro* motility assay observed that decreasing pH from 7.4 to 6.5 slowed actin filament velocity by ~67% at 20˚C (12). This assay was performed with naked actin (i.e. no Tn and Tm), confirming that acidosis is directly impacting myosin's ability to move actin.

The motion of actin filaments in an *in vitro* motility assay are well characterized by a detachment limited model (29). Where the velocity, **v**, of actin filaments is equal to the unitary displacement of one myosin, **d**, divided by the time myosin spends strongly bound to actin, $\mathbf{t_{on}}$, (i.e. $v = d / t_{on}$). Because actin filament velocity is determined by **d** and $\mathbf{t_{on}}$, researchers postulated that acidosis may slow contraction velocity by decreasing **d** and/or increasing $\mathbf{t_{on}}$. However, in conventional *in vitro* motility assays and single fiber studies, **d** and $\mathbf{t_{on}}$ cannot be measured directly.

Thanks to advancements in single molecule techniques the chemo-mechanical parameters responsible for the acidosis-induced decrease in velocity can be measured directly. A study performed by Debold et al. (2008) found that acidosis has no effect on **d**, but increases $\mathbf{t_{on}}$ by three-fold, an increase that can quantitatively account for the 67% decrease in velocity in a motility assay (12). As seen in Figure 2, $\mathbf{t_{on}}$ is dependent on two different biochemical steps, the ADP release step and the rigor lifetime, the latter of which is dependent on the second order ATP binding constant (~2.5×10^6 $M^{-1} \cdot s^{-1}$) (62). Because $\mathbf{t_{on}}$ depends on two different rate constants, further experiments were needed to determine if the acidosis induced increase in $\mathbf{t_{on}}$ was a result of slowed ADP release or slowed ATP binding. By increasing the ATP concentration in the laser trap assay, $\mathbf{t_{on}}$ becomes dominated by the ADP lifetime. At higher concentrations of

ATP, Debold et al. (2008) found that $\mathbf{t_{on}}$ was unchanged under acidic conditions, evidence that the increased $\mathbf{t_{on}}$ was a result of slowed ADP release and not a prolonged rigor lifetime. These findings provide the first direct evidence of the specific step in the crossbridge cycle that likely underlies the decrease in shortening velocity associated with fatigue. Because this study was performed in the absence of regulatory proteins, any affect acidosis has on Tn and Tm is being overlooked. Therefore, the mechanisms that impact actin filament velocity in a Ca^{2+} regulated system needed to be investigated. Studies that performed *in vitro* motility with RTF found a similar down right shift in the velocity-pCa relationship compared to a force-pCa relationship (Figure 1) (15, 40). Thus, in a Ca^{2+} regulated system of motility, acidosis may slow actin filament velocity by limiting the number of cycling crossbridges due to decreased Ca^{2+} sensitivity.

2.4 Summary of the Review

The link between acidosis and skeletal muscle fatigue is well understood. The accumulation of H^+ has both direct and indirect effects on actomyosin interaction (10, 12, 70), the latter being mediated through direct effects on the regulatory proteins Tn and Tm (4, 20, 38, 55). The net result of acidosis is a decrease in RTF Ca^{2+} sensitivity, force and shortening velocity of skeletal muscle fibers. The mechanisms through which acidosis mediates these effects are now becoming clearer. For instance, the decreased Ca^{2+} sensitivity of the RTF associated with acidosis is likely caused by decreased Ca^{2+} affinity of TnC (55). Additionally, researchers have speculated that the transmission of the Ca^{2+} binding signal is inhibited by acidosis; an effect which may be mediated through TnI (4). Tropomyosin has also been implicated in the fatigue process where studies demonstrated that active tension development in fibers was impacted by the Tm isoform (20), and that Ca^{2+} sensitivity is enhanced via rare Tm

mutations (61). The direct effects of acidosis on actomyosin interaction has been studied for longer but recent insights have been made (12) . For instance, acidosis effectively slows the attachment rate of cycling myosin (2, 9), thereby decreasing the number of strongly attached crossbridges. A result that should theoretically decrease force production *in vivo* (28, 67). Additionally, there is evidence that ADP release is slowed under acidic conditions (12). An outcome that provides a compelling explanation for the decreased contraction velocity caused by fatigue *in vivo*.

Despite this overwhelming amount of research, no studies, have yet directly measured how acidosis impacts the mechanics and kinetics of single actomyosin binding events in a Ca^{2+} regulated system. Recent studies have determined how actomyosin interactions are impacted in a Ca^{2+} regulated system in normal pH conditions (16, 30, 39). Due to these advancements, the impact acidosis has on Ca^{2+} regulation can be measured directly at the single molecule level. This will provide unique insights into the mechanisms which lead to decreased RTF Ca^{2+} sensitivity.

2.5 Specific aims & hypothesis

2.5.1 Aim 1: Characterize the direct effects of acidosis on myosin

This proposal is focused on identifying mechanisms which leads to decreased Ca^{2+} sensitivity and isometric tension in muscle fibers. Therefore, to isolate the effects of acidosis on myosin from the effects of acidosis on the RTF, these experiments must be performed with and without regulatory proteins. Acidosis is hypothesized to slow specific steps in the crossbridge cycle (12) and has been shown to decrease actin activated ATPase (71). This suggests that

acidosis might affect steps off actin leading to a decrease in binding frequency at the single molecule level. My hypothesis is that in the single molecule laser trap assay, myosin binding to naked actin (i.e. no Tn or Tm) will occur less frequently at pH 6.5 compared to pH 7.4. A result which could help explain the decreased actin activated ATPase rate as well as the impaired contractile performance of isolated muscle fibers *in vitro*.

2.5.2 Aim 2: Characterize the effects of acidosis on RTF Ca^{2+} sensitivity

Acidosis is known to impact Ca^{2+} sensitivity of the RTF. The mechanisms responsible for this decreased Ca^{2+} sensitivity are thought to be mediated through effects on TnC, TnI and Tm (4, 38, 55, 61). Because the activation state of the RTF impacts actomyosin binding, I hypothesize that the decreased Ca^{2+} sensitivity of the RTF will lead to a decreased actomyosin binding frequency over a range of Ca^{2+} concentrations. Because there will also be binding frequency estimations in an unregulated system, the degree to which acidosis impacts the RTF and myosin can be delineated.

Chapter 3
METHODS

3.1 Protein purification/isolation

Myosin was purified from chicken pectoralis muscle using methods previously described (41). Typically, 95% of the myosin heavy chain (MHC) content within chicken pectoralis is expected to be MHC IIB (69). Once the myosin was purified the protein was combined with 5% sucrose, flash frozen in liquid nitrogen and stored at -80˚C for future use. The quality of the sample was later quantified with the *in vitro* motility assay. If the percent of motile filaments was ≥ 85% and the velocity of sliding actin filaments was ≥ 3 μm/s the sample was considered suitable for further experimentation. On the day of an experiment, myosin was combined with a 2-molar excess of actin and 1 mM ATP in a dead-head spindown as previously described (12).

Actin was purified from chicken pectoralis muscle using methods previously described (54). After purification, a 1 μM sample of actin is fluorescently labeled in a solution of 50% TRITC/Phalloidin and 50% Biotin/Phalloidin. This ratio adequately labeled the filaments while also allowing enough of the biotin linker to bind, so that fluorescently labeled actin would bind to neutravidin coated beads (described in section 3.3).

3.2 Reconstituted thin filaments

Reconstituted thin filaments (RTF) were prepared with methods previously described (30, 39) . Briefly, 1 μM TRITC/Biotin labeled actin was incubated with 0.25 μM Tn and 0.25 μM Tm at 4˚C for 3 hours prior to use. The ionic strength of the solution must be 95 mM KCl and filaments must be incubated for < 3 hours to prevent the formation of actin aggregates, which are unsuitable for the laser trap assay. To ensure complete regulation after incubation, the

velocities of the RTF were assessed in an *in vitro* motility (IVM) assay in the absence of Ca^{2+}. Under these conditions the velocity of actin filaments is zero which indicates the regulatory proteins are intact and properly inhibiting actomyosin interaction.

3.3 - Neutravidin coated beads:

To provide a sticky surface for the RTF, 1 µm diameter silica beads were incubated in 20 µL of 0.167 µM Neutravidin (NAV) overnight. On the day of an experiment excess NAV was rinsed from the silica beads with 1 mL of high salt myosin buffer. This suspension was centrifuged at 13,000 RPM to reform the pellet. The supernatant was discarded, and the NAV coated beads were resuspended in 500 µL of experimental buffer.

3.4 - Three-bead assay:

On the day of an experiment a flow chamber was constructed by laying a 22 X 22 mm coverslip onto a 24 X 50 mm microscope slide and fixing them together with a UV activated adhesive. The larger 24 X 50 mm slide was coated in a 1.0% nitrocellulose film sparsely coated with 3 µm silica beads which served as pedestals for myosin to adhere.

After the chamber was constructed 33 µL of 0.1 µg/mL myosin was injected into the chamber and allowed to adhere to the surface through a 2-minute incubation. After the incubation 33 uL of 7.25 µM BSA was injected into the chamber and incubated for 8 minutes. The BSA blocks the surface by filling in the gaps between myosin molecules. Blocking with BSA will help minimize unwanted non-specific electrostatic interactions. After the 8-minute incubation three, 33 µL shots of experimental buffer were injected into the flow chamber. This step washes out all excess BSA while equilibrating the flow chamber to the desired

experimental conditions (i.e. pH, [ATP], pCa and ionic strength). Once the chamber is completed, 100 µL of final buffer, which consists of 0.02 uM TIRT-C labeled RTF, 100nM excess Tn and Tm as well as 0.5 µL of NAV coated beads, was made. Finally, 20 µL of final buffer is injected into the flow chamber.

3.5 - Data acquisition:

Once the bead-actin-bead geometry has been achieved (Figure 5,) the actin filament was pretensioned. This was accomplished by slowly moving the position of the two traps away from each other as to pull compliance out of the system. Once the RTF was sufficiently rigid and the system sufficiently stiff (~0.02 pn/nm, determined through the equipartition method (51)) the myosin coated surface was sampled. The bead actin bead assembly was then lowered toward the surface over a 3 µm silica bead. The RTF was then scanned over the pedestal with a piezo controlled stage until the quadrant photodiode (QD) begins to show the presence of events (transient drops in signal variance). At that point, 5 second recordings of the bead position were captured every 5 seconds. Because the trap is weak in the z-axis, the RTF was repositioned above the pedestal bead every 1-2 minutes to ensure consistent RTF and myosin proximity.

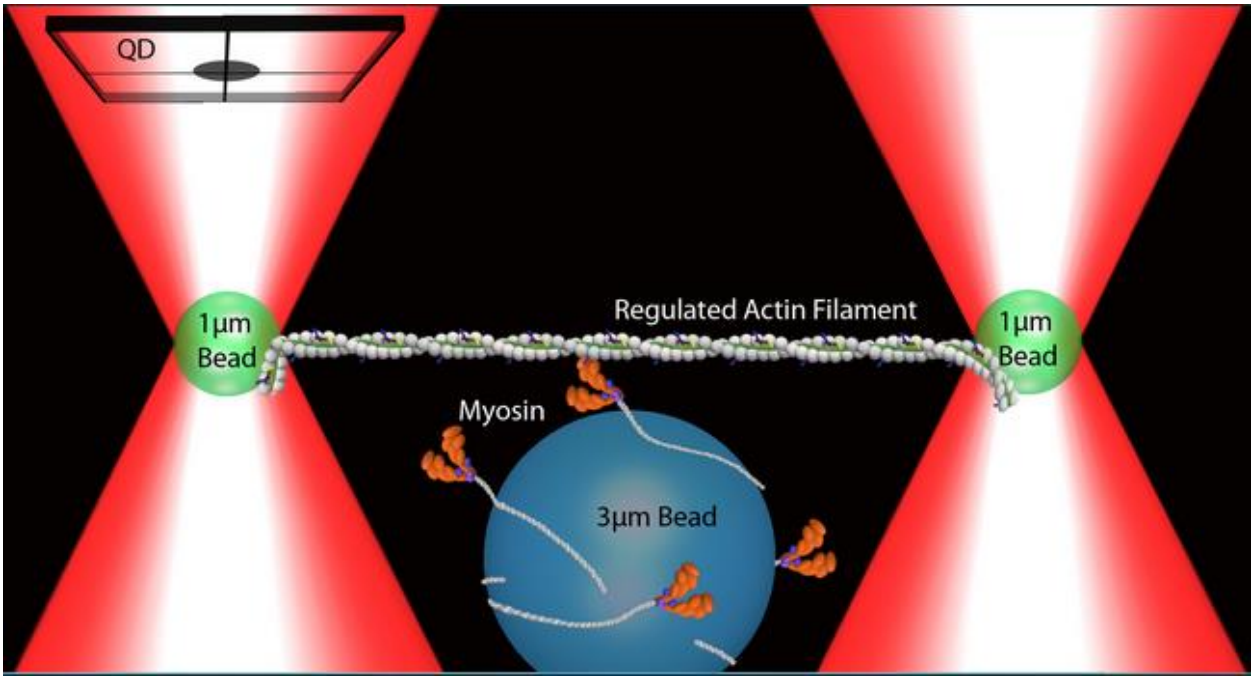

Figure 5 A schematic of the three-bread laser trap assay. The red cones indicate the laser traps which are holding 1 µm silica beads (green). The RTF, white, is fixed to the silica beads via a NAV – Biotin linkage. The QD is in the top left corner of the figure, this sensor detects changes in the bead position at a frequency of 5 kHz.

3.7 Data analysis

3.7.1 Page Method

The raw data recordings were analyzed with a custom Python program previously described (39) which is based off of a modified version of Page's method previously described (34, 52, 68). Briefly, this method takes advantage of the underlying probability density function (PDF) of the position of a trapped bead when myosin is bound to actin and when myosin is detached from actin (Figure 6). This PDF was then used to calculate a log-odds

ratio, where values above zero indicate a high probability of attachment and values less than zero indicate a high probability of detachment. A zero-threshold cumulative sum was then

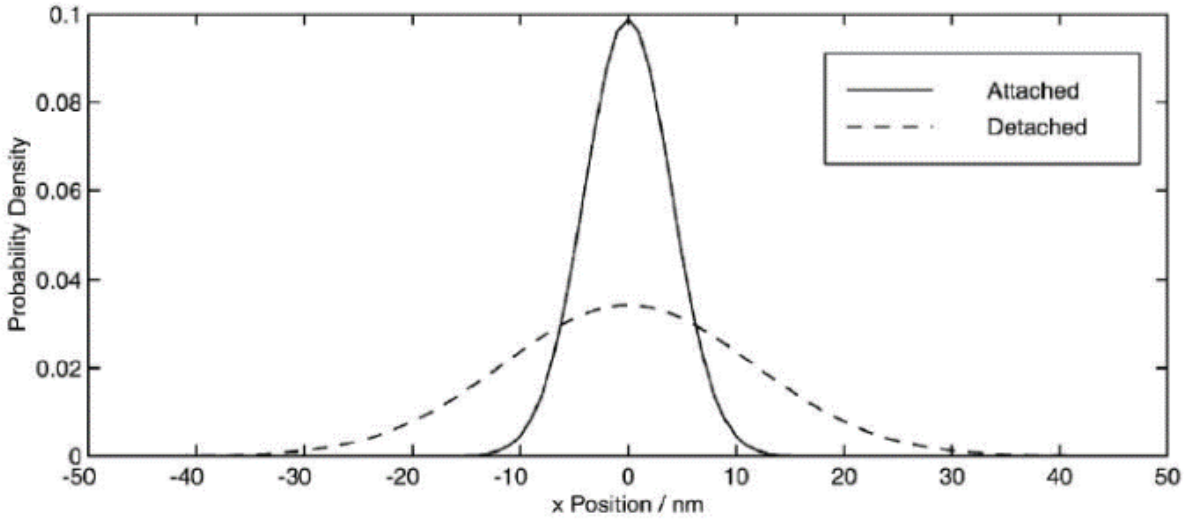

Figure 6 Probability density function. This figure shows that the mean position of the bead in both the unattached and detached states is zero. However, the distance that an attached bead explores is approximately 20 nm, while the distance that a detached bead explores is close to 60 nm (34).

calculated from the log odds ratio. The cumulative sum rapidly increases above zero when the probability of attachment is high and rapidly sum to zero when the probability of attachment is low (Figure 7B). Since the peak value of the cumulative sum corresponds to the duration of an event, a predetermined threshold which corresponds to event lifetimes of 10ms is used for this analysis.

All raw data traces were analyzed in groups of contiguous recordings, i.e. each 5 second recording was concatenated with a custom Python script. These chunks of contiguous recordings will be treated as one continuous record, from which binding frequency, average displacement and event duration will be determined. If a raw data trace starts and/or ends within the middle of an event, those records were truncated in order to remove those parts of

the record. To determine if pH affects actomyosin binding frequency, a repeated measures ANOVA was used with an α of 0.05. The data was compared between pH conditions (6.5 vs 7.4). The same analysis was used to evaluate pH-induced effects on τ_{on} and d.

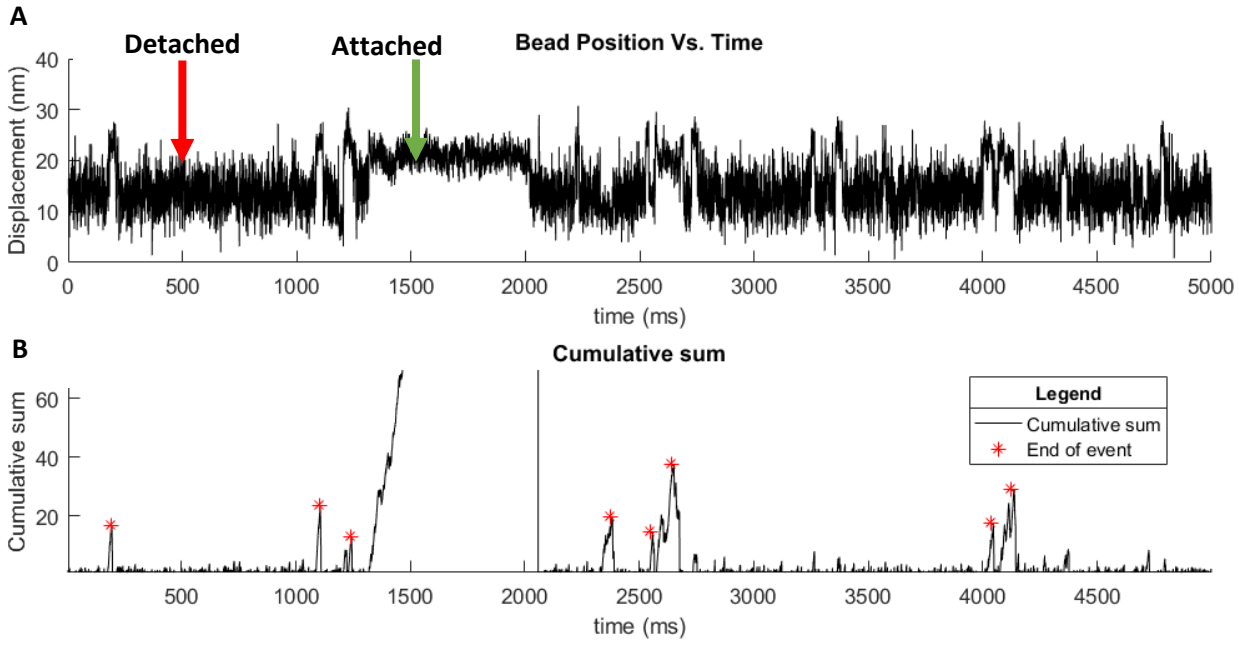

Figure 7 Page method analysis. A. Raw recording of a trapped bead in the laser trap assay. When actin is detached from myosin the signal from the QPD is highly variant, red arrow. During an acto-myosin binding event there is a transient drop in signal variance with a subsequent bead displacement, green arrow. **B.** The corresponding cumulative sum of the raw trace after Page analysis with the y-scale cutoff to retain clarity. The cumulative sum is a logarithmically scaled dimensionless value. During long events, the cumulative sum will increase for a greater period, leading to a high cumulative sum. During shorter events, the cumulative sum will not reach as high a peak. This means that shorter events become difficult to separate from Brownian noise within the data. The red asterisks indicate the end of an event.

Shortly after data collection was completed, the Page Method was determined to be an unsuitable analysis technique because of the heavy parameterization required to optimize the event detection algorithm. For example, the window width required for processing the data, and the cumulative sum threshold used to trigger event detection are both user determined parameters. Due to the natural variation in data quality, i.e. the signal to noise ratio, these parameters needed to be adjusted for almost every record. Despite this heavy amount of user input, the Page Method was not able to reliably detect events (Figure 8). This method routinely

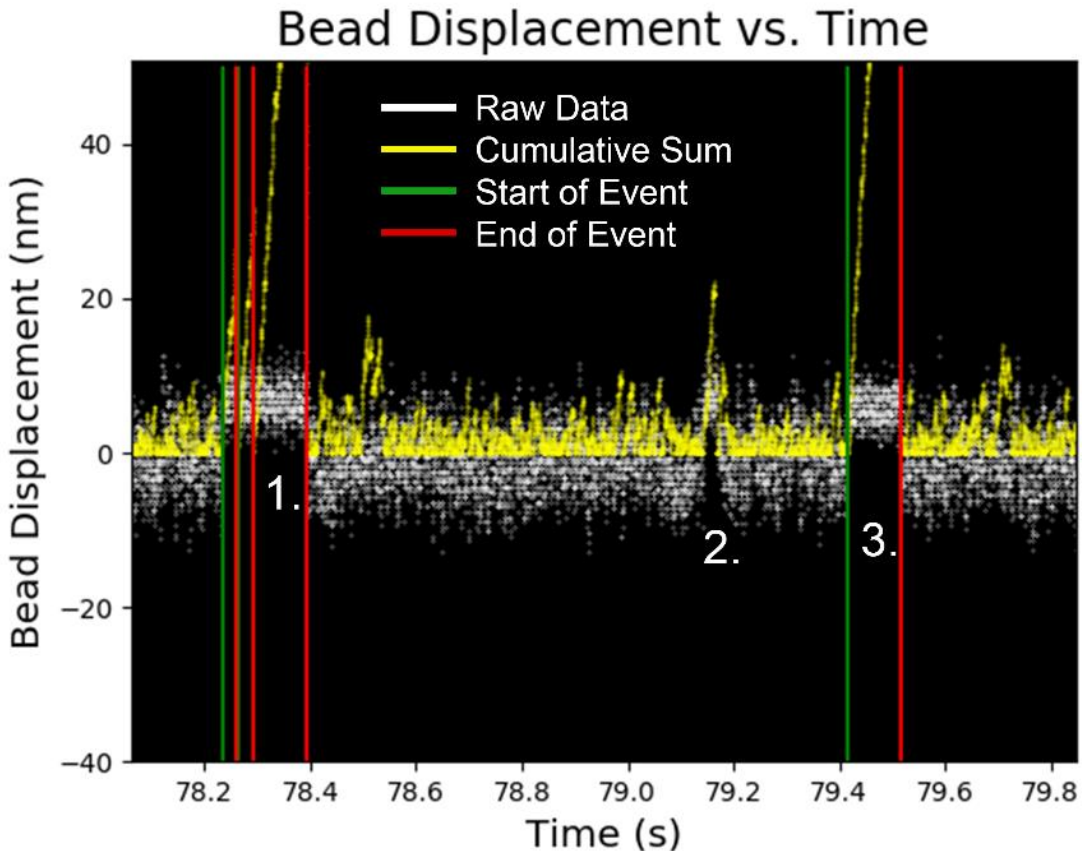

Figure 8 Detection with Page method. An example recording demonstrating the results of the Page method. Note that the first event, labeled 1., is counted as an event three times. Additionally, event number 2, which appears to be of much shorter duration, is not counted at all. In this recording, event 3 is the only event that is detected reliably.

counted a single event as multiple events, regularly missed short events, and often provided false positives. Some of these problems can be ameliorated by modifying the algorithm parameters, but this can lead to poor reproducibility as well as experimental bias. For this reason, another analysis method was used.

3.7.2 Mean Variance Method

Raw Data (Figure 7A) were analyzed using the mean-variance (MV) analysis technique which involves routinely calculating the mean and variance of the raw displacement records with variably sized windows (e.g. 16 ms – 800 ms). The window is advanced by half of its width over the entire displacement record and the mean and variance of the raw signal is calculated each time the window is advanced. Each point in the record is plotted in a 3-D histogram (Figure 9A) with the third dimension indicating the number of observations binned within a specific mean variance value. This means that if a 5 second record, sampled at 5 kHz, is filtered with the 16ms window, the resulting 3-D histogram will contain 625 data points.

The 3-D histograms clearly display two populations; a baseline population, which represents periods of time myosin is detached from actin and an event population, which represents periods of time myosin is strongly bound to actin. Sampling the raw data with variably sized windows provides a measure of the rate at which the density of the event population decays (Figure 9B). By analyzing the rate of decay of the event population, it is possible to determine the average time myosin spends strongly bound to actin, as well as the number of events within a raw data record. Therefore, event density (ρ) as a function of the window width (τ_ω) was then plotted and fit with a mono-exponential decay, Equation 1:

$$\textbf{Eq 1. } \boldsymbol{\rho(\tau_\omega) = \tau_{on} N e^{\frac{(1-\tau_\omega)}{\tau_{on}}}}$$

with τ_{on} representing the time myosin spends strongly bound to actin, and *N* the number of binding events within a record. All event densities were summed within a given condition (up to 30 minutes of raw data) before the fitting process (Appendix A), therefore the fit determines τ_{on} and N over an extended period. The total number of events, N, is divided by the total record time to determine the event frequency for each condition.

In order to evaluate the Ca^{2+} sensitivity of actomyosin binding, the event frequency data were fit with the Hill equation, Equation 2:

$$\textbf{Eq 2. } \boldsymbol{f(pCa) = Vmin + \frac{Vmax - Vmin}{1 + \frac{pCa50^n}{pCa}}}$$

with V_{min} and V_{max} representing the maximum and minimum activity, pCa_{50} representing the pCa to achieve 50% activation and n represents the Hill slope (23). The magnitude of the displacements (i.e. size of the powerstroke) were also determined using the MV analysis technique (26).

Because our frequency and τ_{on} measurements are based on one estimate from equation 1 (Appendix A), a two-way ANOVA cannot be used to test for significant differences. Therefore, a paired t-test was used determined if pH influenced binding frequency and τ_{on} across all pCa values. A two-way ANOVA was used to determine if there was an interaction between pCa and pH in respect to step size.

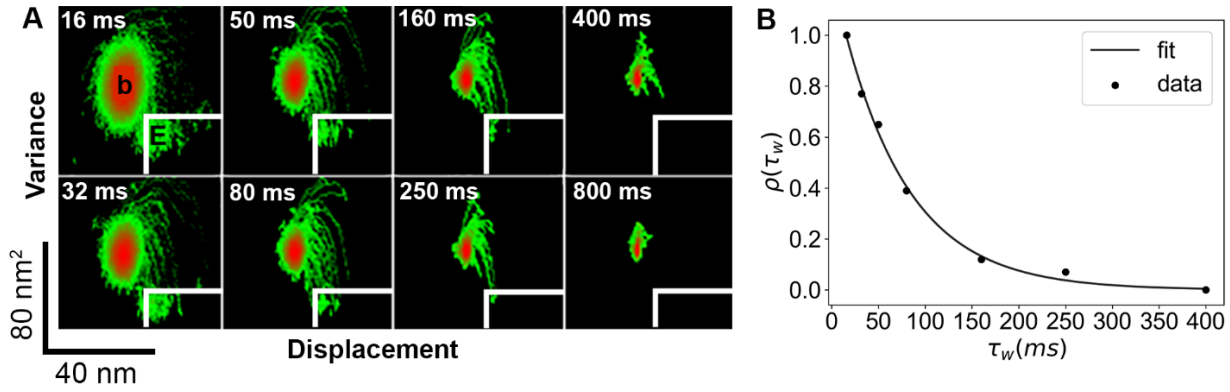

Figure 9 Using window widths to construct event density plots. A. An example of the MV-analysis after one raw data record was filtered via a running window of varying size. The size of the window width, in milliseconds, is displayed in the top left corner of each MV-histogram. Note the strong baseline population, b, in the 16 ms window histogram along with the event population, E, which is outlined with the solid white lines. In order to go from MV-analysis shown in A, to the event density plot shown in B. **B,** the volume of events captured in each window, i.e. within the solid white lines, was normalized to the peak volume of events captured within the 16 ms window (Appendix A) and then fit to equation 1. The 16 ms window was chosen as the minimum sized window because this provides the optimum signal to noise ratio given the stiffness of the laser trap (34).

Preliminary visual inspection of the raw data reveals that the actomyosin binding frequency appears to be dependent on Ca^{2+} sensitivity (Figure 10), consistent with previous results (39). However, any pH dependence of binding frequency, step size and event duration cannot be discerned with a crude visual inspection. Moreover, the short, ~ five second time scale displayed in Figure 10, cannot capture differences in binding frequency at the lowest pCa, where event frequency is expected to be extremely low (30). To achieve more quantitative analysis of myosin's step size, event duration and binding frequency, all the data were analyzed

with the Mean-Variance method.

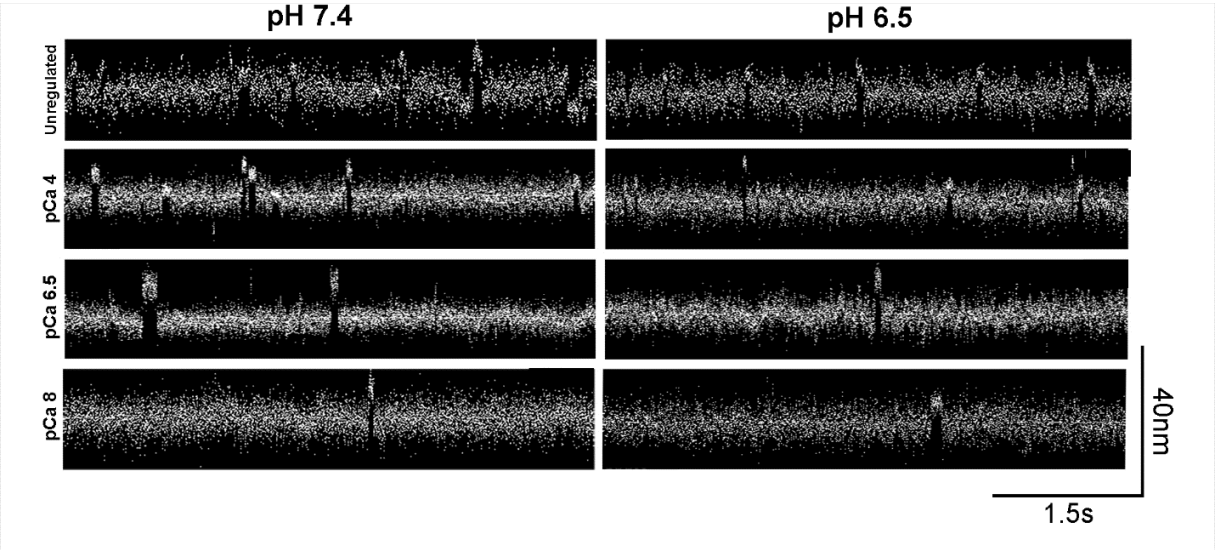

Figure 10 Representative raw actin filament displacement records. 5sec. samples of regulated actin filament displacement vs. time at 3 pCa levels and both pH's. The raw records show binding events, characterized by a short reduction in the signal noise and displacements from the mean when myosin is bound to the filament.

Chapter 4
RESULTS

After obtaining the event duration and myosin's step size with Mean-Variance analysis (Figure 11 and 12), a series of paired t-tests revealed that pH has a significant effect on τ_{on}, but only at pCa 8, 7, 6.5, 5, and in the unregulated condition (Figure 11A). However, because there is no evidence that pCa should impact strongly bound lifetime (30, 39), the τ_{on} data were grouped by pH. When τ_{on} was grouped by pH, a paired t-test found no significant difference in τ_{on} between pH 7.4 and pH 6.5 (Figure 11B). Additionally, although a two-way ANOVA determined there is a significant interaction between pH and pCa for myosin's step size (Figure 12B), when the step sizes were grouped by pH (Figure 12C), a paired t-test found no significant difference in step size between pH 7.4 and pH 6.5 (Figure 12C), consistent with previous results (12).

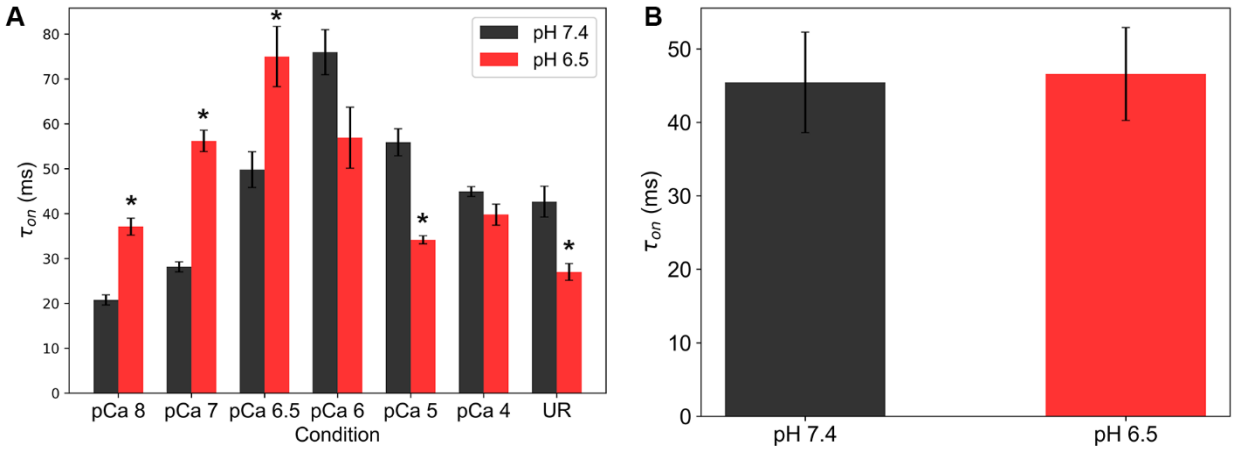

Figure 11 τ_{on} summary. A. The event duration results separated by pCa and pH. Bars represent τ_{on} as predicted from equation 1. Because all event densities were summed before they were fit to equation 1, τ_{on} represents the average lifetime over minutes of data (Appendix A, Table 2),

error bars represent the SEM as determined from one fit therefore $n_{observations} = 1$ for all bars in A. A paired t-test, with $\alpha = 0.05$ was used with to check if within a condition (i.e. pCa), pH affected τ_{on}. * indicates that τ_{on} is significantly different at pH 6.5 compared to pH 7.4. **B**. The τ_{on} results grouped by pH. Each bar represents the average τ_{on} for pH 7.4 and pH 6.5 with error bars representing the SEM. $n_{observations} = 7$ for both bars in B. A significant interaction was determined if $p < 0.05$. UR represents the "Unregulated" condition, i.e. without regulatory proteins.

The frequency of single actomyosin binding events were dependent on Ca^{2+} concentration (Figure 13), consistent with previous findings (39). Additionally, acidosis did not significantly affect the frequency of actomyosin binding events at saturating pCa (Figure 13). However, at sub-saturating pCa, e.g. pCa 6, acidosis reduced the frequency of single actomyosin interactions by almost 50%. Indeed, dropping the pH from 7.4 to 6.5 decreased the single molecule binding frequency at all sub-saturating pCa, from pCa 6 to pCa 8 (Figure 13). The greatest difference was observed at pCa 6.5 where the frequency was decreased by ~75%.

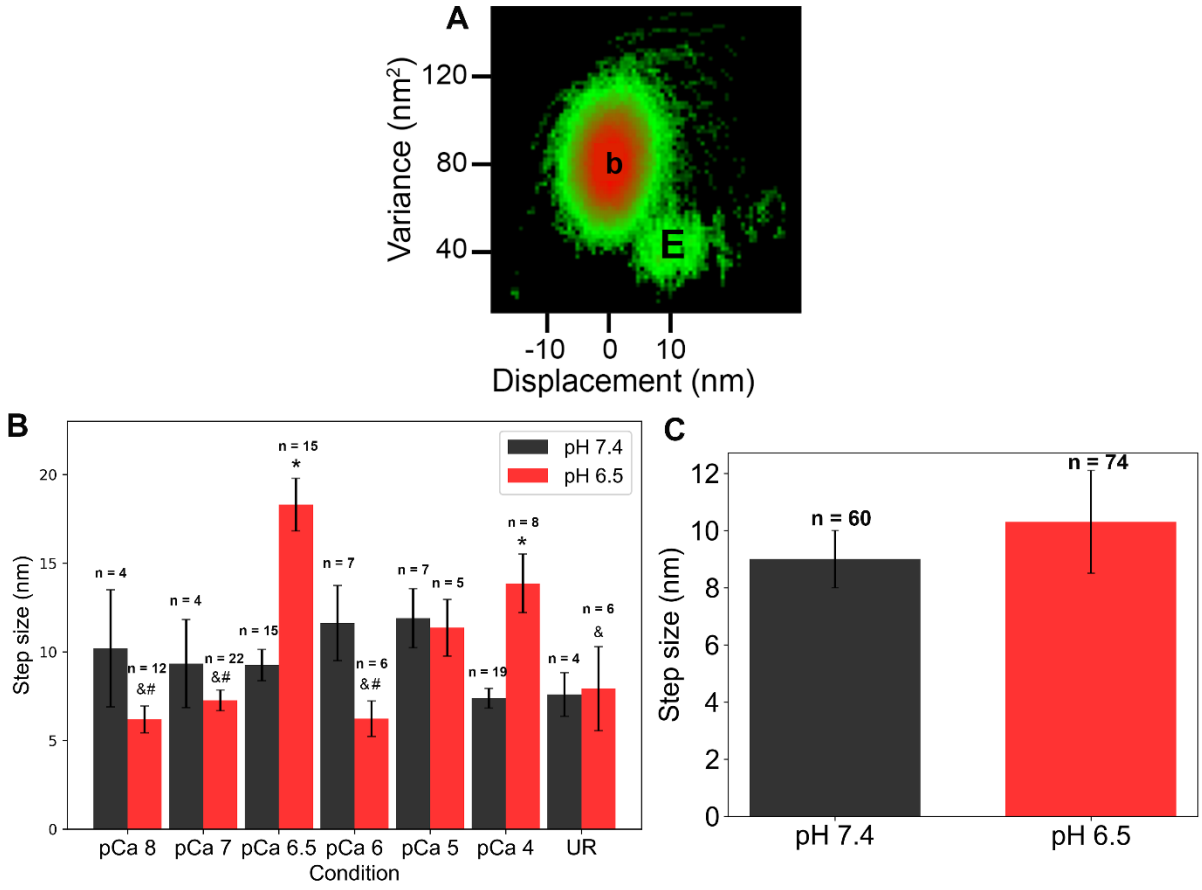

Figure 12 Myosin's step size summary. A. A single 3-D histogram after analyzing one raw data record with the 16 ms window. Both the baseline population, b and the event population E are well fit in the displacement dimension by the sum of two gaussians. Once the event and baseline populations have been deconvolved through the fitting process, the event population step size can then be determined by taking the difference between the mean of the event population from the mean of the baseline population (26). **B**. The step size results separated by pCa and pH. Bars represent the average displacement calculated over n number of raw data records for each condition and error bars represent the SEM. A two-way ANOVA was then used to determine if there was a significant interaction between both pH and pCa with respect to myosin's step size. *, Indicates significantly different, $P < 0.05$, from pH 7.4 within a given pCa.

&, Indicates significantly different, P < 0.05, from pH 6.5 – pCa 6.5. #, Indicates significantly different, P < 0.05, from pH 6.5 – pCa 4. **C**. The step size results grouped by pH. A paired t-test with α = 0.05 was used with to check if there was a difference in step size between pH 7.4 and pH 6.5, with n equal to the number of raw records contributing to the step size average and error bars represent the SEM. See Appendix B for a note on step size calibration.

In addition to the effect low pH has on frequency at sub-saturating pCa, the pCa_{50} of the Event frequency is increased at low pH (Table 1), an indication that acidosis is decreasing the Ca^{2+} sensitivity of the RTF, which is consistent with previous work (18, 40). Most interestingly, because acidosis did not affect the frequency of binding in the absence of Tn and Tm (Figure 13), the acidosis induced depression in event frequency is not likely caused by a direct effect on myosin.

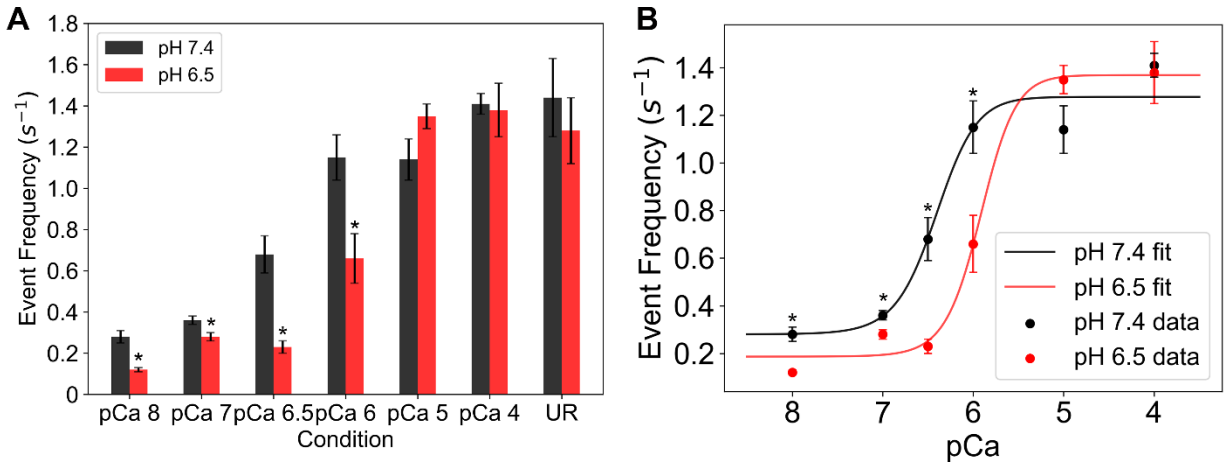

Figure 13 Event frequency results. A. A bar chart showing the event frequency for all the measured conditions. A paired t-test was used to test differences in event frequency across pH in a fixed pCa condition. * Indicates significantly different, P < 0.05, from pH 7.4. B The event frequency results fit to the Hill equation.

	Vmax (s^{-1} ± SEM)	**Vmin** (s^{-1} ± SEM)	**pCa_{50}**	**Hill Slope**
pH 7.4	1.27 ± 0.10	0.29 ± 0.12	6.41 ± 0.14 *	1.45 ± 1.20
pH 6.5	1.37 ± 0.06	0.19 ± 0.06	5.92 ± 0.08 *	1.48 ± 1.30

Table 1: Event frequency vs. pCa fit results. A table showing the fit results when the event frequency vs. pCa data are fit to the Hill equation, equation 2. A paired t-test with α set to 0.05 was used to determine a difference, if any, between the fit parameters of the pH 7.4 vs. pH 6.5 data. * Indicates significantly different, $P < 0.05$, pH 7.4.

Chapter 5
DISCUSSION

Here the molecular mechanisms underlying the acidosis-induced decrease in contractile performance of muscle were investigated, with specific emphasis put on the combined effects of acidosis and decreased Ca^{2+} release from the SR (Figure 1). The results presented in this study show that acidosis profoundly inhibits actomyosin binding, but only at sub-saturating pCa (Figure 13). This suggests that the acidosis-induced rightward shift in the force-pCa relationship observed in single muscle fibers (18, 49, 55) may be caused by slowing the rate at which a single myosin head binds to the actin filament and this is likely mediated through competitive inhibition of Ca^{2+} binding to Tn. Despite acidosis having a Ca^{2+} dependent effect on myosin's on rate, the step size and strongly bound lifetime appear to be unchanged by acidosis. Additionally, because acidosis did not significantly reduce myosin's binding frequency in the absence of Tn and Tm (Figure 13A), acidosis does not likely mediate its depressive effects by directly impacting myosin, but rather the effect of acidosis is mediated through the regulatory proteins, specifically Tn.

5.1 Acidosis does not affect myosin's strongly bound lifetime or step size

Previous work demonstrated acidosis decreases unloaded shortening velocity in muscle fibers up to 30% at 15˚ C (31, 35). While purified protein studies showed that decreasing pH from 7.4 to 6.5 slows actin filament velocity by ~67% at 20˚C in an *in vitro* motility assay (12). Debold et al., 2008 postulated a molecular mechanism whereby acidosis slows myosin's ADP release rate thereby increasing myosin's strongly bound lifetime by 33% at saturating ATP concentrations (~1 mM ATP). An outcome that provides a compelling explanation for the

decreased contraction velocity caused by fatigue *in vivo*. In this study, however, acidosis did not appear to change myosin's strongly bound lifetime, τ_{on} (Figure 11B). This may seem to contradict Debold et al., 2008, however, because acidosis does not impact myosin's rigor lifetime, any change to the short lived, ~4 ms ADP lifetime (3) would be difficult to detect. This is because random Brownian motion of the trapped bead limits the precision of our τ_{on} measurement to ~ 6 - 7 ms (34, 68). Lastly, acidosis did not appear to impact myosin's step size (Figure 12B and C), which is consistent with previous results (12).

5.2 Acidosis impacts TnC-Ca^{2+} binding

In muscle, Tn and Tm regulate actomyosin binding through a Ca^{2+} dependent process. Calcium released from the SR binds to the Ca^{2+} binding domain of Tn (TnC), which induces a conformational change (Figure 4) leading to an azimuthal rotation of Tm on the surface of actin (27, 58, 65) to reveal the myosin binding sites (Figure 3). After these binding sites are revealed, myosin can strongly bind to actin (23). At saturating pCa, the Ca^{2+} binding sites on TnC are fully occupied, and thus attachment can occur at the highest frequency, which in this assay is 1.4 times per second (Figure 13). In contrast, at sub-saturating pCa (pCa 6.0 to pCa 8) TnC is likely not fully bound with Ca^{2+}, thus actomyosin binding is partially inhibited (58), which results in a decrease in the event frequency observed at sub-maximal Ca^{2+} levels. Therefore, the present observation demonstrates that acidosis inhibits actomyosin binding, but only at sub-maximal pCa. This suggests that acidosis affects the ability of Ca^{2+} to bind to TnC and produce the conformational changes in the inhibitory subunit of Tn (TnI) that allows Tm to reveal the myosin binding sites on actin. Because acidosis did not decrease actomyosin binding frequency at saturating Ca^{2+}, the function of Tn and Tm is likely intact at low pH once TnC is fully bound with

Ca^{2+}. This is consistent with a mechanism proposed by Parsons et al., (1997) in which acidosis interferes with Ca^{2+} binding to TnC thereby decreasing Ca^{2+}-sensitivity in muscle fibers. Indeed, our fit results from the Hill equation demonstrate that the pCa_{50} is increased in response to acidosis (Table 1) demonstrating that acidosis decreases RTF Ca^{2+}-sensitivity.

The pronounced rightward shift in the binding frequency-pCa relationship (Fig. 14A) is strikingly similar to the acidosis-induced rightward shift in the force-pCa relationship observed in single muscle fibers (18), (Figure 14B). This suggests that the present findings provide the molecular basis for the acidosis-induced reduction in force in muscle fibers at sub-saturating pCa. If so, these findings indicate that acidosis reduces force in muscle fibers at sub-saturating pCa by slowing the rate at which the first myosin molecule attaches strongly to the actin filament. The decrease in the apparent attachment rate of myosin to actin observed in this experiment demonstrates that force in muscle may be reduced because less cross-bridges are attached at any given sub-saturating pCa. Although the force of an individual cross-bridge may be reduced by acidosis (46), the size of myosin's powerstroke was unaffected by pH in these experiments, suggesting myosin might be generating a similar force (Figure 12C). Thus, the decrease in force seen in fibers at sub-saturating pCa may be primarily due to a decrease in myosin's attachment rate, and this depression in myosin's attachment rate is caused by the inability of TnC to bind to Ca^{2+} at low pCa.

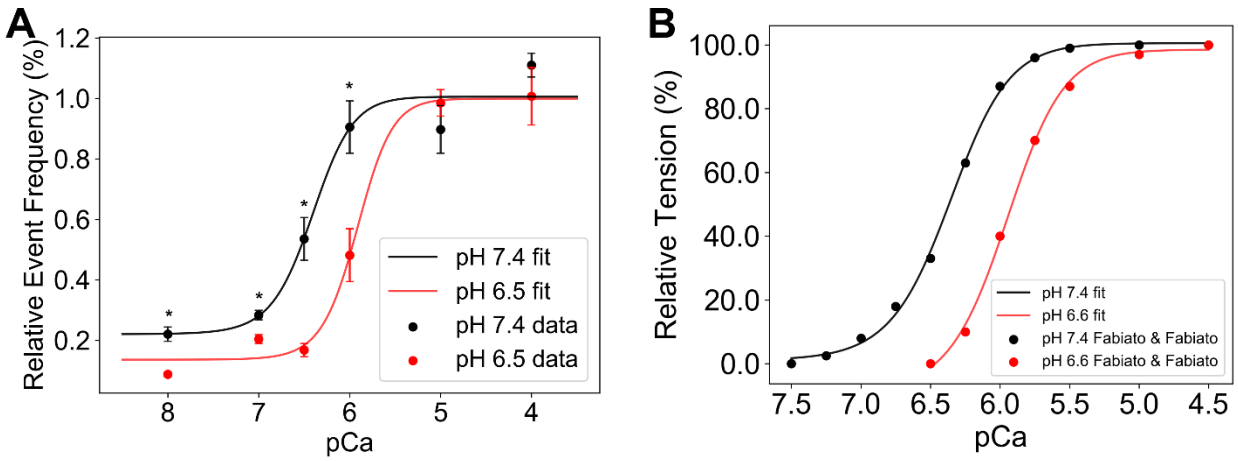

Figure 14 Comparing single molecule data to fiber data. A. A normalized event frequency vs. pCa curve. The data were normalized within a pH condition by dividing each data point by the predicted Vmax based off the fit results in Table 1. B. Replotted relative tension data from (18). The strong rightward shift is apparent at both the single molecule and single muscle fiber level.

Despite acidosis leading to a pronounced rightward shift in the force-pCa / event frequency-pCa relationship (Figure 14A and 14B respectively), acidosis does not appear to have any effect on the Hill slope of the force-pCa relationship in fibers (18, 49). This suggests that the complex mechanisms responsible for the cooperative aspect of thin filament activation (23), including myosin strong-binding's influence on the position of Tm on actin (11) and TnC-Ca^{2+} binding cooperativity (25), are unaffected by acidosis.

In this assay there was never more than one myosin head interacting with an actin filament. Therefore, the Hill slope measured in this experiment only includes TnC Ca^{2+}- binding cooperativity. Thus, no conclusion of how acidosis impacts myosin strong binding cooperativity can be made. However, acidosis does not seem to impair TnC Ca^{2+}-binding cooperativity, meaning that transmission of the Ca^{2+} binding signal is likely unaffected by acidosis. Therefore,

although acidosis may be impacting TnC-Ca^{2+} binding, once there is enough Ca^{2+} in solution, i.e. above the pCa_{50} (Table 1), TnC will become saturated with Ca^{2+} and the TnC-Ca^{2+} binding signal will not be attenuated. These data provide further support for the notion that acidosis affects the affinity of Tn for Ca^{2+} (Figure 15).

5.3 Conclusion

Here skeletal muscle fatigue was successfully simulated at the single molecule level by measuring the effect of acidosis on actomyosin interaction in a Ca^{2+} dependent manner. These findings provide important mechanistic insight into the molecular basis of fatigue because the drop in pH investigated here is similar to the changes observed in vivo (7) and because the pCa where acidosis had the biggest impact in these experiments reflects the well-documented decrease in intracellular pCa that occurs during fatigue (36).

The decrease in pH alone is not thought to decrease isometric tension while at 30˚C (56), however when low pH is combined with a decrease in intracellular Ca^{2+}, that occurs later in fatigue (1) the combined response may account for a significant portion of the loss in force-generating capacity during fatigue-induced acidosis. The present data suggests that the ability of TnC to bind Ca^{2+} is compromised under acidic conditions due to H^+ competition . As a result, the regulatory unit remains deactivated at sub-maximal pCa (Figure 15A). Therefore, TnI never removes its inhibition on Tm. Consequently, the rate of cross-bridge formation decreases, causing less cross-bridges to be attached at any given time. These data provide a compelling explanation for the observed decrease in tension at sub-saturating pCa in muscle fibers (18, 50). Additionally, because peak isometric tension isn't effected by acidosis at 30˚C (56) it's unsurprising there was no observed change in frequency at saturating pCa in this experiment.

These data help to provide a molecular level explanation that can account for the loss of force caused by acidosis during fatigue at sub-saturating pCa, while simultaneously explaining how force is unchanged at saturating pCa. While there are certainly other mechanisms that contribute to the loss of force during fatigue, including inorganic phosphate (P_i) (15, 49, 71) these data provide critical and novel molecular insight into the mechanisms through which acidosis might reduce force late in the fatigue process.

5.4 Future Directions

Although the results from this study provide a molecular level explanation for the observed decrease in force of muscle fibers in response to acidosis (10, 18) (Figure 14), future studies should expand on this work to provide a more complete mechanism. For instance, because there was only one head available to bind to an actin filament at any given time, any influence that acidosis has on myosin strong binding cooperativity is ignored in this study. Therefore, performing this experiment with an mini-ensemble of myosin (14) would allow researchers to determine the effect, if any, acidosis has on myosin strong binding cooperativity. Additionally, this type of study would allow for the measurement of force, which cannot be done easily with the current trapping software. Lastly, because we are proposing that competition exists between H^+ and Ca^{2+} for TnC binding sites, the depression in frequency should worsen as pH levels continue to decrease. Therefore, more work should be completed to investigate how H^+ ions are impacting TnC-Ca^{2+} affinity.

In addition, because TnC-Ca^{2+} binding was not measured directly, the depression in binding frequency observed may be caused by acidosis inhibiting the transmission of the TnC-Ca^{2+} binding signal to TnI. Although these data suggest otherwise, this experiment could be

performed with different TnC and or TnI constructs to determine which structural elements in Tn mediate the effects of acidosis. Such information would be invaluable in gaining a more completing understanding of the mechanisms which mediate the depressive effects of acidosis on muscle. This can aid in the development of small molecules and other treatments to attenuate muscle fatigue in clinical populations.

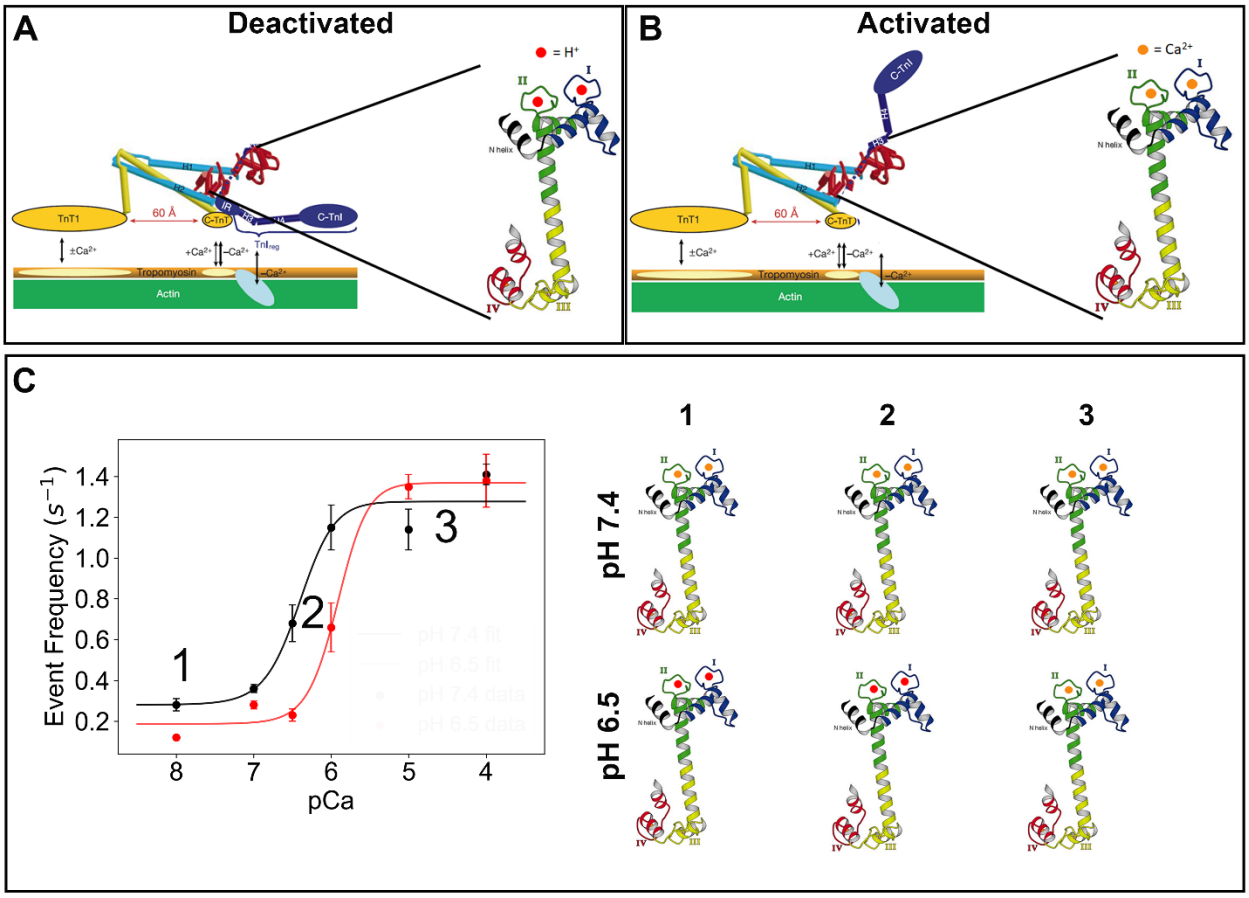

Figure 15 Conceptual model. A model describing the binding frequency results. **A.** A diagram of the 3-subunit Tn complex while in the deactivated state (i.e. in the absence of Ca^{2+} (orange circles) and/ or in the presence of H^{+} (red circles)). The bold black lines surrounding the red section of the Tn complex (TnC) point toward the crystal structure of TnC with the putative Ca^{2+} binding sites labeled I and II (blue and green respectively). Note that in the deactivated state,

TnI (blue) is interacting Tm and actin, causing Tm to remain in the blocked state therefore myosin and actin cannot bind. Tm will remain in the blocked state if TnC isn't bound to Ca^{2+} or, as our data suggests (Figure 14A), if there are high levels of H^+ ions. **B**. The same diagram in **A**, however TnC is occupied with Ca^{2+} which allows C-TnI to interact with TnC allowing Tm to move away from the blocked state therefore myosin and actin can interact. This panel represents a properly functioning Tn complex. **C**. The event frequency results from Figure 13A. Labeled with a 1, 2 and 3. On the right, 6 representations of TnC occupied with either Ca^{2+} (orange circles) or H^+ (red circles) depending on the pH. Under normal pH conditions, and at very low Ca^{2+}, labeled 1, the probability of both Ca^{2+} binding sites I and II being occupied are low, however TnC Ca^{2+} binding can still occur, albeit infrequently. At pH 6.5-pCa 8, H^+ concentration is approximately 15-fold higher than the Ca^{2+} concentration. Therefore, the probability of H^+ ions occupying sites I and II is higher and because H^+ doesn't appear to elicit the same conformational change in TnC that Ca^{2+} does (55), the Tn complex remains in the deactivated state and Tm remains in the blocked state more often, therefore driving down binding frequency. At higher pCa (e.g pCa 6) under normal pH conditions, the probability of TnC being occupied with two Ca^{2+} ions is much higher, leading to an enhancement in binding frequency. However, at pH 6.5-pCa 6, labeled 2 H^+ concentration is approximately 5-fold less than Ca^{2+} ion concentration. Therefore, the probability of both sites being occupied with Ca^{2+} begins to increase compared to the low pCa condition. However, there is still an opportunity for H^+ competition. Lastly, under saturating pCa, labeled 3, at pH 7.4, the Ca^{2+} binding sites in TnC are saturated with Ca^{2+} which is why binding frequency is highest. Additionally, at pH 6.5 Ca^{2+} concentration is approximately 20-fold

higher than H^+ concentration. Therefore, the Ca^{2+} binding sites are more likely to be occupied with Ca^{2+} than with H^+ and binding frequency recovers to normal pH levels.

APPENDIX A
DETERMINING EVENT DENSITIES

Before the event density, $\rho(\tau_\omega)$ is calculated, the number of positive observations observed for a given window width (e.g. 50 ms) were summed across all raw data records (e.g. 5 raw data records) within a condition (e.g. pH 7.4 - pCa 4), equation 1.

$$\textbf{Eq. 1}\ N(\tau_\omega) = \sum_{i=1}^{i=j} n_i$$

Where j represents the j^{th} raw data record and n_i represents the number of positive observations. Once the total number of positive observations, $N(\tau_\omega)$, are accumulated for a given condition, this result is normalized, Equation 2, to the total number of observations observed within the 16 ms window, $N(\tau_{16})$, thereby providing a measure of the event density over every raw data record within a given condition. Table 2 shows the number of minutes recorded for each condition.

$$\textbf{Eq. 2}\ \rho(\tau_\omega) = N(\tau_\omega) \,/\, N(\tau_{16})$$

	pCa 8	**pCa 7**	**pCa 6.5**	**pCa 6**	**pCa 5**	**pCa 4**	**Unregulated**
pH 7.4	6.8 min	10.3 min	11.2 min	4 min	10.3 min	37.4 min	9.7 min
Ph 6.5	26.3 min	31.4 min	18 min	5 min	10.8 min	11 min	17.2 min

Table A1 Minutes of raw data collected. Values represent the total amount of raw data, in minutes, collected for all 14 conditions.

APPENDIX B
STEP SIZE CALIBRATION

In order to convert the raw voltage signal from the Quadrant Photodiode, (QD), a standard displacement curve must be constructed (Figure 16). This is accomplished by fixing a 1 um glass bead to the surface of the flow cell. Once a bead that is strongly attached to the surface is found, the trap is brought close to the surface and the stuck bead is placed into the center of the trap via the piezo controlled stage. At that time, the piezo controlled stage is rapidly moved (~ 4ms) as to cause the 1 um bead to be displaced a known distance from the center of the trap, in this case 50 um (Figure 16A). This process of rapidly displacing the stuck bead from the center of the trap is repeated up to 4 times so that the stuck bead experiences a large displacement (~200 um) from the center of the trap. When the bead is moved in this manner the response of QD should be linear (Figure 16B), but If the bead is displaced by a greater distance the response of the QD begins to lose its linearity. Therefore, the goal of the step size calibration is to characterize the linear response of the QD.

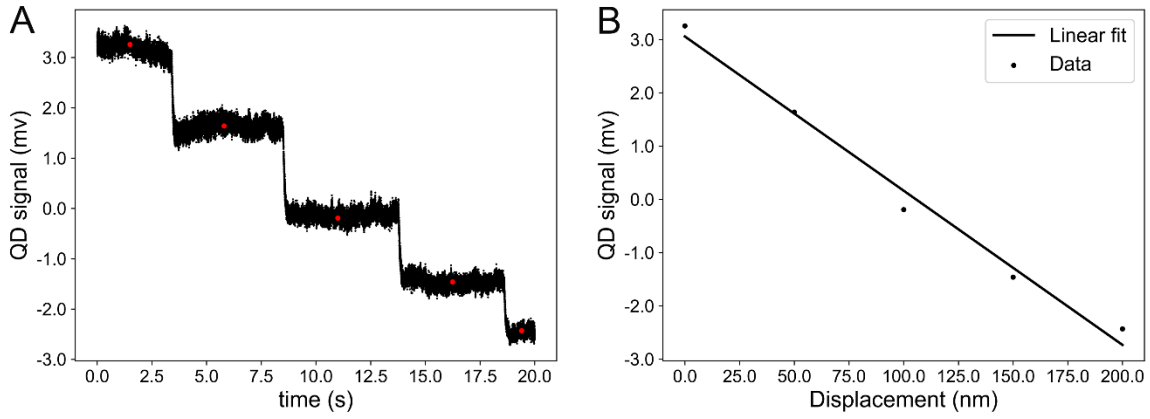

Figure B1 Creating standard displacement curve. A. The QD signal in mv as a 1 um bead is displaced from the center of the trap in 50 um increments. Notice that each step occurs on a

very short time scale (~4 ms) and that with each step the change in the QD signal is roughly equal in magnitude. The red dots in A represent the average QD signal calculated over the flat, stable portions of the raw trace. These averages were then plotted in B and fit to a linear function of the form $y = mx + b$, where $|m|$ is the conversion factor between QD voltage and bead displacement.

Originally, I assumed that the result from this step size calibration would be stable day after day, however the displacements obtained for the pH 6.5-pCa 6.5 condition (Figure 12B) are abnormally high for single actomyosin interactions. This means either, the step size calibration is not consistent day after day, or the raw data collected for that condition was not single molecule. However, because binding frequency is expected to increase when there is more than one myosin head available to bind (30, 39), I would expect to see an increased binding frequency for the pH 6.5 – pCa 6.5 condition, but this was not the case (Figure 13). Additionally, further inspection of the raw data provided me with no reason to believe that there are multiple heads interacting with the actin filament at any given time. Therefore, the likely hood that the step size calibration can change day to day is high. Therefore, performing the step size calibration each day is likely best practice.

REFERENCES

1. **Allen DG**, **Lamb GD**, **Westerblad H**. Skeletal Muscle Fatigue: Cellular Mechanisms. *Physiol Rev* 88: 287–332, 2008.

2. **Bagshaw CR**, **Trentham DR**. The characterization of myosin-product complexes and of product-release steps during the magnesium ion-dependent adenosine triphosphatase reaction. *Biochem J* 141: 331–349, 1974.

3. **Baker JE**, **Brosseau C**, **Joel PB**, **Warshaw DM**. The Biochemical Kinetics Underlying Actin Movement Generated by One and Many Skeletal Muscle Myosin Molecules. *Biophys J* 82: 2134–2147, 2002.

4. **Ball KL**, **Johnson MD**, **Solaro RJ**. Isoform Specific Interactions of Troponin I and Troponin C Determine pH Sensitivity of Myofibrillar Ca2+ Activation. *Biochemistry* 33: 8464–8471, 1994.

5. **Bremel RD**, **Weber A**. Cooperation within Actin Filament in Vertebrate Skeletal Muscle. *Nature New Biol* 238: 97, 1972.

6. **Brown JH**, **Cohen C**. Regulation of muscle contraction by tropomyosin and troponin: how structure illuminates function. *Adv Protein Chem* 71: 121–159, 2005.

7. **Broxterman RM**, **Layec G**, **Hureau TJ**, **Amann M**, **Richardson RS**. Skeletal muscle bioenergetics during all-out exercise: mechanistic insight into the oxygen uptake slow component and neuromuscular fatigue. *J Appl Physiol Bethesda Md 1985* 122: 1208–1217, 2017.

8. **Chase PB**, **Kushmerick MJ**. Effects of pH on contraction of rabbit fast and slow skeletal muscle fibers. *Biophys J* 53: 935–946, 1988.

9. **Chock SP**. The mechanism of the skeletal muscle myosin ATPase. III. Relationship of the H+ release and the protein absorbance change induced by ATP to the initial Pi burst. *J Biol Chem* 254: 3244–3248, 1979.

10. **Cooke R**, **Franks K**, **Luciani GB**, **Pate E**. The inhibition of rabbit skeletal muscle contraction by hydrogen ions and phosphate. *J Physiol* 395: 77–97, 1988.

11. **Craig R**, **Lehman W**. Crossbridge and tropomyosin positions observed in native, interacting thick and thin filaments11Edited by W. Baumeister. *J Mol Biol* 311: 1027–1036, 2001.

12. **Debold**, **Beck SE**, **Warshaw DM**. Effect of low pH on single skeletal muscle myosin mechanics and kinetics. *Am J Physiol-Cell Physiol* 295: C173–C179, 2008.

13. **Debold EP**, **Fitts RH**, **Sundberg CW**, **Nosek TM**. Muscle Fatigue from the Perspective of a Single Crossbridge. *Med Sci Sports Exerc* 48: 2270–2280, 2016.

14. **Debold EP**, **Walcott S**, **Woodward M**, **Turner MA**. Direct Observation of Phosphate Inhibiting the Force-Generating Capacity of a Miniensemble of Myosin Molecules. *Biophys J* 105: 2374–2384, 2013.

15. **Debold**, **Turner MA**, **Stout JC**, **Walcott S**. Phosphate enhances myosin-powered actin filament velocity under acidic conditions in a motility assay. *Am J Physiol-Regul Integr Comp Physiol* 300: R1401–R1408, 2011.

16. **Desai R**, **Geeves MA**, **Kad NM**. Using fluorescent myosin to directly visualize cooperative activation of thin filaments. *J Biol Chem* 290: 1915–1925, 2015.

17. **Ebashi S**. Excitation-Contraction Coupling and the Mechanism of Muscle Contraction. *Annu Rev Physiol* 53: 1–17, 1991.

18. **Fabiato A**, **Fabiato F**. Effects of pH on the myofilaments and the sarcoplasmic reticulum of skinned cells from cardiace and skeletal muscles. *J Physiol* 276: 233–255, 1978.

19. **Farah CS**, **Reinach FC**. The troponin complex and regulation of muscle contraction. *FASEB J* 9: 755–767, 1995.

20. **Fujita H**, **Ishiwata S**. Tropomyosin Modulates pH Dependence of Isometric Tension. *Biophys J* 77: 1540–1546, 1999.

21. **Galińska-Rakoczy A**, **Engel P**, **Xu C**, **Jung H**, **Craig R**, **Tobacman LS**, **Lehman W**. Structural Basis for the Regulation of Muscle Contraction by Troponin and Tropomyosin. *J Mol Biol* 379: 929–935, 2008.

22. **Godt RE**, **Nosek TM**. Changes of intracellular milieu with fatigue or hypoxia depress contraction of skinned rabbit skeletal and cardiac muscle. *J Physiol* 412: 155–180, 1989.

23. **Gordon AM**, **Homsher E**, **Regnier M**. Regulation of Contraction in Striated Muscle. *Physiol Rev* 80: 853–924, 2000.

24. **Gordon AM**, **Regnier M**, **Homsher E**. Skeletal and Cardiac Muscle Contractile Activation: Tropomyosin “Rocks and Rolls.” *Physiology* 16: 49–55, 2001.

25. **Grabarek Z**, **Grabarek J**, **Leavis PC**, **Gergely J**. Cooperative binding to the Ca2+-specific sites of troponin C in regulated actin and actomyosin. *J Biol Chem* 258: 14098–14102, 1983.

26. **Guilford WH**, **Dupuis DE**, **Kennedy G**, **Wu J**, **Patlak JB**, **Warshaw DM**. Smooth muscle and skeletal muscle myosins produce similar unitary forces and displacements in the laser trap. *Biophys J* 72: 1006–1021, 1997.

27. **Houdusse A**, **Love ML**, **Dominguez R**, **Grabarek Z**, **Cohen C**. Structures of four Ca2+-bound troponin C at 2.0 Å resolution: further insights into the Ca2+-switch in the calmodulin superfamily. *Structure* 5: 1695–1711, 1997.

28. **Huxley F**. Muscle structure and theories of contraction. *Prog Biophys Biophys Chem* 7: 255–318, 1957.

29. **Huxley HE**. Sliding filaments and molecular motile systems. *J Biol Chem* 265: 8347–8350, 1990.

30. **Kad NM**, **Kim S**, **Warshaw DM**, **VanBuren P**, **Baker JE**. Single-myosin crossbridge interactions with actin filaments regulated by troponin-tropomyosin. *Proc Natl Acad Sci U S A* 102: 16990–16995, 2005.

31. **Karatzaferi C**, **Franks-Skiba K**, **Cooke R**. Inhibition of shortening velocity of skinned skeletal muscle fibers in conditions that mimic fatigue. *Am J Physiol Regul Integr Comp Physiol* 294: R948-955, 2008.

32. **Kent-Braun JA**, **Fitts RH**, **Christie A**. Skeletal muscle fatigue. *Compr Physiol* 2: 997–1044, 2012.

33. **Kentish JC**. Combined inhibitory actions of acidosis and phosphate on maximum force production in rat skinned cardiac muscle. *Pflugers Arch* 419: 310–318, 1991.

34. **Knight AE**, **Veigel C**, **Chambers C**, **Molloy JE**. Analysis of single-molecule mechanical recordings: application to acto-myosin interactions. *Prog Biophys Mol Biol* 77: 45–72, 2001.

35. **Knuth ST**, **Dave H**, **Peters JR**, **Fitts RH**. Low cell pH depresses peak power in rat skeletal muscle fibres at both 30 degrees C and 15 degrees C: implications for muscle fatigue. *J Physiol* 575: 887–899, 2006.

36. **Lee JA**, **Westerblad H**, **Allen DG**. Changes in tetanic and resting [Ca2+]i during fatigue and recovery of single muscle fibres from Xenopus laevis. *J Physiol* 433: 307–326, 1991.

37. **Li XE**, **Tobacman LS**, **Mun JY**, **Craig R**, **Fischer S**, **Lehman W**. Tropomyosin position on F-actin revealed by EM reconstruction and computational chemistry. *Biophys J* 100: 1005–1013, 2011.

38. **Liou YM**, **Chang JCH**. Differential pH Effect on Calcium-Induced Conformational Changes of Cardiac Troponin C Complexed with Cardiac and Fast Skeletal Isoforms of Troponin I and Troponin T. *J Biochem (Tokyo)* 136: 683–692, 2004.

39. **Longyear T**, **Walcott S**, **Debold EP**. The molecular basis of thin filament activation: from single molecule to muscle. *Sci Rep* 7: 1822, 2017.

40. **Longyear TJ**, **Turner MA**, **Davis JP**, **Lopez J**, **Biesiadecki B**, **Debold EP**. Ca++-sensitizing mutations in troponin, Pi, and 2-deoxyATP alter the depressive effect of acidosis on regulated thin-filament velocity. *J Appl Physiol* 116: 1165–1174, 2014.

41. **Margossian SS**, **Lowey S**. [7] Preparation of myosin and its subfragments from rabbit skeletal muscle. In: *Methods in Enzymology*. Academic Press, p. 55–71.

42. **Maron BJ**, **Roberts WC**, **Epstein SE**. Sudden death in hypertrophic cardiomyopathy: a profile of 78 patients. *Circulation* 65: 1388–1394, 1982.

43. **McKillop DF**, **Geeves MA**. Regulation of the interaction between actin and myosin subfragment 1: evidence for three states of the thin filament. *Biophys J* 65: 693–701, 1993.

44. **McKillop DFA**, **Geeves MA**. Regulation of the acto·myosin subfragment 1 interaction by troponin/tropomyosin. Evidence for control of a specific isomerization between two acto·myosin subfragment 1 states. *Biochem J* 279: 711–718, 1991.

45. **Merton P. A.** Voluntary strength and fatigue. *J Physiol* 123: 553–564, 1954.

46. **Metzger JM**, **Moss RL**. Greater hydrogen ion-induced depression of tension and velocity in skinned single fibres of rat fast than slow muscles. *J Physiol* 393: 727–742, 1987.

47. **Miller RG**, **Boska MD**, **Moussavi RS**, **Carson PJ**, **Weiner MW**. 31P nuclear magnetic resonance studies of high energy phosphates and pH in human muscle fatigue. Comparison of aerobic and anaerobic exercise. *J Clin Invest* 81: 1190–1196, 1988.

48. **Narita A**, **Yasunaga T**, **Ishikawa T**, **Mayanagi K**, **Wakabayashi T**. Ca2+-induced switching of troponin and tropomyosin on actin filaments as revealed by electron cryo-microscopy1 1Edited by A. Klug. *J Mol Biol* 308: 241–261, 2001.

49. **Nelson CR**, **Debold EP**, **Fitts RH**. Phosphate and acidosis act synergistically to depress peak power in rat muscle fibers. *Am J Physiol-Cell Physiol* 307: C939–C950, 2014.

50. **Nelson CR**, **Fitts RH**. Effects of low cell pH and elevated inorganic phosphate on the pCa-force relationship in single muscle fibers at near-physiological temperatures. *Am J Physiol-Cell Physiol* 306: C670–C678, 2014.

51. **Neuman KC**, **Nagy A**. Single-molecule force spectroscopy: optical tweezers, magnetic tweezers and atomic force microscopy. *Nat Methods* 5: 491–505, 2008.

52. **Page ES**. CONTINUOUS INSPECTION SCHEMES. *Biometrika* 41: 100–115, 1954.

53. **Palmer S**, **Kentish JC**. The role of troponin C in modulating the Ca2+ sensitivity of mammalian skinned cardiac and skeletal muscle fibres. *J Physiol* 480: 45–60, 1994.

54. **Pardee JD**, **Spudich JA**. Chapter 18 Purification of Muscle Actin. In: *Methods in Cell Biology*, edited by Wilson L. Academic Press, p. 271–289.

55. **Parsons B**, **Szczesna D**, **Zhao J**, **Slooten GV**, **Kerrick WGL**, **Putkey JA**, **Potter JD**. The effect of pH on the Ca2+ affinity of the Ca2+ regulatory sites of skeletal and cardiac troponin C in skinned muscle fibres. *J Muscle Res Cell Motil* 18: 599–609, 1997.

56. **Pate E**, **Bhimani M**, **Franks-Skiba K**, **Cooke R**. Reduced effect of pH on skinned rabbit psoas muscle mechanics at high temperatures: implications for fatigue. *J Physiol* 486: 689–694, 1995.

57. **Phillips GN**, **Chacko S**. Mechanical properties of tropomyosin and implications for muscle regulation. *Biopolymers* 38: 89–95, 1996.

58. **Pirani A**, **Vinogradova MV**, **Curmi PMG**, **King WA**, **Fletterick RJ**, **Craig R**, **Tobacman LS**, **Xu C**, **Hatch V**, **Lehman W**. An Atomic Model of the Thin Filament in the Relaxed and Ca2+-Activated States. *J Mol Biol* 357: 707–717, 2006.

59. **Sandow A**. Excitation-Contraction Coupling in Muscular Response. *Yale J Biol Med* 25: 176–201, 1952.

60. **Schmidt WM**, **Lehman W**, **Moore JR**. Direct Observation of Tropomyosin Binding to Actin Filaments. *Cytoskelet Hoboken NJ* 72: 292–303, 2015.

61. **Sheehan KA**, **Arteaga GM**, **Hinken AC**, **Dias FA**, **Ribeiro C**, **Wieczorek DF**, **Solaro RJ**, **Wolska BM**. Functional effects of a tropomyosin mutation linked to FHC contribute to maladaptation during acidosis. *J Mol Cell Cardiol* 50: 442–450, 2011.

62. **Siemankowski RF**, **Wiseman MO**, **White HD**. ADP dissociation from actomyosin subfragment 1 is sufficiently slow to limit the unloaded shortening velocity in vertebrate muscle. *Proc Natl Acad Sci* 82: 658–662, 1985.

63. **Swartz DR**, **Moss RL**. Influence of a strong-binding myosin analogue on calcium-sensitive mechanical properties of skinned skeletal muscle fibers. *J Biol Chem* 267: 20497–20506, 1992.

64. **T. Finer J**, **M. Simmons R**, **Spudich J**. Single myosin molecule mechanics: Piconewton forces and nanometre steps. 1994.

65. **Takeda S**, **Yamashita A**, **Maeda K**, **Maéda Y**. Structure of the core domain of human cardiac troponin in the Ca^{2+}-saturated form. *Nature* 424: 35, 2003.

66. **Thompson LV**, **Balog EM**, **Riley DA**, **Fitts RH**. Muscle fatigue in frog semitendinosus: alterations in contractile function. *Am J Physiol-Cell Physiol* 262: C1500–C1506, 1992.

67. **VanBuren P**, **Guilford WH**, **Kennedy G**, **Wu J**, **Warshaw DM**. Smooth muscle myosin: a high force-generating molecular motor. *Biophys J* 68: 256S-259S, 1995.

68. **Veigel C**, **Bartoo ML**, **White DCS**, **Sparrow JC**, **Molloy JE**. The Stiffness of Rabbit Skeletal Actomyosin Cross-Bridges Determined with an Optical Tweezers Transducer. *Biophys J* 75: 1424–1438, 1998.

69. **Verdiglione R**, **Cassandro M**. Characterization of muscle fiber type in the pectoralis major muscle of slow-growing local and commercial chicken strains. *Poult Sci* 92: 2433–2437, 2013.

70. **Westerblad H**, **Allen DG**. Changes of myoplasmic calcium concentration during fatigue in single mouse muscle fibers. *J Gen Physiol* 98: 615–635, 1991.

71. **Woodward M**, **Debold EP**. Acidosis and Phosphate Directly Reduce Myosin's Force-Generating Capacity Through Distinct Molecular Mechanisms. *Front Physiol* 9, 2018.